Effect of defect structures on chemically active surfaces: A continuum approach

Anthony P. Peirce
Program in Applied and Computational Mathematics, Princeton University, Princeton, New Jersey 08544

Herschel Rabitz
Department of Chemistry, Princeton University, Princeton, New Jersey 08544
(Received 13 November 1987)

A continuum approach is used to analyze the effect of defect structures on chemically active surfaces. The model comprises a linear diffusion equation with adsorption and desorption in which the defect structures are represented by nonlinear localized-reaction terms. The issue of multiple steady states and stability is treated, and a novel procedure is outlined that uses conformal mapping to derive stability criteria for these localized-reaction diffusion equations. This conformal mapping procedure also provides insight into how the various physical processes affect the stability of the system. A class of reactive-trapping models is considered in which defects are assumed to act as sinks of material that ultimately desorbs as a chemical product. Other features included in the model are nonlinear enhanced reactivity with concentration, and saturation effects. The continuum assumption is tested by direct comparison with a discrete reactive-trapping model and found to be a remarkably good approximation, even when the number of interdefect sites is as low as 20. We investigate the effect of relative defect locations on the balance between the desorptive processes that take place on the surface. The effect of defect locations on desorption is analyzed by considering symmetry-breaking perturbations to the defects in a periodic lattice. Two regimes of desorption are identified depending on the level of adsorption on the surface and the defect spacing. (i) Competitive: Defects that are moved closer by the perturbation *compete* for material, which reduces the trapping efficiency of the defect lattice and increases the bulk desorption rate; by considering the bulk desorption rate to be a function of the defect locations, we conclude that the situation of equally spaced defects is a local minimum of this function. (ii) Cooperative: Defects that are moved closer by perturbation in this regime act *cooperatively* to reduce the saturation level locally, which enhances the trapping efficiency of the defect lattice and reduces the bulk desorption rate. In this complex environment of competing physical effects it would be difficult to determine the dominant process without the analysis presented here. In order to determine whether these phenomena persist when the defects undergo finite random perturbations, we solve the continuum equations numerically using the boundary-element technique. The phenomena identified by the small perturbation case do persist when finite defect variations are considered.

I. INTRODUCTION

There is considerable fundamental and practical interest in the role of chemically active surface defect structures. Practical catalytic reactors are likely to contain active surfaces with high coverages of defect structures due to faulting or foreign substances. Theoretical and experimental investigations on the atomic scale are just beginning. Another fruitful approach is to use continuum modeling to analyze these phenomena on a more macroscopic scale. This approach provides access to the powerful analytic and numerical tools that have been developed to solve continuum phenomena. This paper is concerned with the continuum approach to defect structures on catalytic surfaces.

Recently some analytic models of diffusion, adsorption and/or desorption on surfaces, and reaction at defects have been considered. On the atomic level, Serri *et al.*[1] used a stepped surface model to analyze the desorption kinetics of NO from Pt(111). Examples of continuum models are as follows: the effect of a single defect site has been analyzed by means of a linear boundary-condition-type reaction model;[2] an effective-medium approach has been used to consider the reaction between a single species and a set of randomly distributed reaction sites;[3] the steady states of a system involving diffusion, reaction, and multiple species have been determined by means of the multigrid method and by using elongated Gaussian representations of defect structures;[4] the latter model has been extended to include time-dependent effects, and the influence of a poisoning effect by the product species on the diffusion and reaction processes has been considered.[5]

Continuum diffusion-localized-reaction models have also been considered in other contexts: far from equilibrium phenomena at local sites have been investigated for a single active site in an infinite medium,[6] the number and stability of steady states for a two-site problem exhibiting activation and inhibition have been considered,[7] cooperative instability phenomena have been investigated for arrays of catalytic sites,[8] and the reactive effect of membrane bound enzymes[9–11] and enzyme particles in stirred reacting fluids[12] have also been investigated.

In the present work we use the continuum diffusion-localized-reaction model to investigate the effect of reactive trapping by defects on a catalytic surface. We consider issues of multiple steady states and linear stability and we outline a novel procedure that uses conformal mapping to determine sufficient conditions for linear stability. This technique provides useful insight into the way in which various physical processes influence stability by altering the shape and extent of the stability region. Stability criteria are derived using this technique, and are applied later in the paper when the reactive-trapping models are considered.

The continuum assumption is assessed by direct comparison with a discrete system in which a process of reactive trapping takes place at defect sites. The continuum model is seen to be remarkably good even when the number of atomic sites between defect sites is as low as 20.

A study is made of the effect of the relative locations of the defects upon the desorption processes on the surface. We consider the effect of small symmetry-breaking perturbations to the defect locations in a periodic array on the balance between the desorption associated with the bulk of the surface and the desorptive effect of the reactive defects.

A number of interesting phenomena are observed, including (i) a regime of *competitive* behavior between the defects; and (ii) a regime of *cooperative* behavior between the defects. It is important to obtain a detailed quantitative account of all the competing physical effects that contribute to the desorptive processes. Reliance on physical intuition alone will often be unsatisfactory owing to the fact that the dominance of various competing effects cannot be assessed. The analysis performed in this paper uses a novel perturbation approach. This perturbation procedure is quite general in that it applies for a wide class of reactive-trapping models and can also be used to analyze situations in which different physical processes take place at the defects.

We explore numerically the effect of finite random perturbations to defect locations on the bulk desorption rate using the boundary-element technique.[13,14] We demonstrate that the effect of finite random perturbations to a uniform lattice in the competitive regime increases the bulk desorption rate. Statistical evidence is presented for the claim that the bulk desorption rate considered as a function of the defect locations has a global minimum when the defects are equally spaced. A similar verification of the small perturbation findings in the cooperative regime is also performed by considering finite random perturbations to defect locations.

In this study we consider only competitive or cooperative defect phenomena for one-dimensional surfaces. These phenomena have been explored on two-dimensional surfaces in another study.[13]

The paper is organized as follows. Section II introduces the governing equations of the continuum defect model. In Sec. III we consider the issue of multiple steady states and stability, and outline a procedure to derive stability criteria using conformal mapping. In Sec. IV we analyze the continuum model of reactive trapping by defects. The validity of the continuum assumption is investigated by comparing the continuum reactive-trapping model to a discrete system in which reactive trapping occurs at defects. Having validated the continuum assumption, the continuum model is used to analyze the effect of the location of defects on the balance between the desorption processes on the surface. A periodic array of defects is considered and the effect of small symmetry-breaking perturbations on the desorption processes is examined. Conditions are established for competitive and cooperative behavior due to perturbations. In Sec. V the effect of finite random perturbations to defects is investigated using the boundary-element technique. In Sec. VI we discuss the results of the analysis. Finally, in order to provide continuity, the end of each major section will provide a summary and relevant comments.

II. GOVERNING EQUATIONS

A. Initial boundary-value problem for linear diffusion and localized nonlinear reaction

The equations governing the diffusion, adsorption-desorption, and localized reaction are taken to be[6]

$$\frac{\partial \mathbf{u}}{\partial t}=\underline{D}\frac{\partial^2 \mathbf{u}}{\partial x^2}-\underline{\Omega}\mathbf{u}+\sum_{l=1}^{L}\mathbf{R}_l(\mathbf{u})\delta(x-x_l)+\mathbf{f} \quad \text{for } x,x_l\in(x_0,x_N)\ . \tag{2.1}$$

Here $\mathbf{u}(x,t)\in\mathbb{R}^{+S}$ is a vector with positive-valued components representing the concentrations of the S different species, $\underline{D}$ is a matrix of diffusion coefficients, $\underline{\Omega}$ is a matrix representing desorption or linear bulk reaction, $\mathbf{R}_l$ is the rate term due to reactions taking place at the active site x_l, and $\mathbf{f}(x,t)$ is the incident flux. In this paper we assume that the bulk is homogeneous so that $\underline{D}$ and $\underline{\Omega}$ are constant and that the bulk processes are decoupled so that $\underline{D}$ and $\underline{\Omega}$ are diagonal.

In order to be able to determine the solution $\mathbf{u}$ of (2.1) we prescribe an initial condition

$$\mathbf{u}(x,0)=\mathbf{u}^0(x)\ , \tag{2.2a}$$

and appropriate boundary conditions of the general form:

$$\left[\underline{\alpha}_r\frac{\partial}{\partial x}+\underline{\beta}_r\right]\mathbf{u}(x_r,t)=\mathbf{g}_r(t) \quad \text{for } r=0 \text{ and } N\ . \tag{2.2b}$$

Here $\mathbf{g}_r$ is a specified function. As was the case with the bulk, we assume that the boundary conditions are decoupled so that $\underline{\alpha}_r$ and $\underline{\beta}_r$ are diagonal. Hence the only coupling in the equations governing the various species occurs through the generally nonlinear reaction term $\mathbf{R}_l$.

Physically, these equations represent localized reactions that occur on a number of parallel chemically active "lines" or steps on a two-dimensional surface in which linear diffusion and adsorption-desorption are taking place. In Sec. IV A we will demonstrate that (2.1) and (2.2) form a continuum model of defect sites on a catalytic surface. Equations (2.1) and (2.2) also provide a one-dimensional model for a more general problem comprising a surface on which adsorption-desorption and linear

diffusion are taking place, while generally nonlinear reaction processes may occur at localized defects in the form of curves on the surface. Similarly, in three dimensions an array of active curved surface planes can be envisioned. Models of localized reactions occurring in a bulk medium have also been considered in the context of membrane bound enzymes,[9-11] cooperative instability phenomena in arrays of catalytic sites,[8] and enzyme particles and other heterogeneities in stirred reacting fluids.[12]

B. Alternative "jump-condition" form

It is possible to rewrite (2.1) in an alternative form if we assume that $\mathbf{u}, \mathbf{f} \in C^0(x_0, x_N)$. We integrate (2.1) over each of the intervals $(x_l-\varepsilon, x_l+\varepsilon)$, $l=1,2,\ldots,L$ in turn letting $\varepsilon \to 0^+$ in each case. An application of the mean-value theorem for integrals yields the following conditions:

$$\underline{D}\left[\frac{\partial \mathbf{u}}{\partial x}\right]_{x=x_l} = -\mathbf{R}_l(\mathbf{u})\,|_{x=x_l}, \quad l=1,2,\ldots,L\ . \tag{2.3}$$

Here

$$\left[\frac{\partial \mathbf{u}}{\partial x}\right]_{x=x_l} := \lim_{\varepsilon\to 0^+}\left[\frac{\partial \mathbf{u}}{\partial x}(x_l+\varepsilon,t)-\frac{\partial \mathbf{u}}{\partial x}(x_l-\varepsilon,t)\right].$$

The initial boundary-value problem (2.1) and (2.2) can now be replaced by the linear partial differential equation (PDE) obtained by setting $\mathbf{R}_l \equiv \mathbf{0}$ in (2.1) and by requiring that the solution should satisfy not only (2.2) but also the additional jump conditions (2.3). This alternative form emphasizes the fact that we have a linear differential equation, the solution of which is subject to nonlinear ancillary conditions. These ancillary conditions reduce to boundary conditions in some special cases. For example, we could assume that the solution $\mathbf{u}$ is constant throughout (x_0, x_N) except for a single subinterval $[x_l, x_{l+1}]$. In this case the jump conditions that apply at x_l and x_{l+1} reduce to derivative boundary conditions.

III. MULTIPLE STEADY-STATE SOLUTIONS AND STABILITY

The existence of multiple steady-state solutions for diffusion-localized-reaction systems and their stability properties have been investigated by a number of authors. For example, Bimpong-Bota *et al.*[6] investigated the number and stability of steady states for the Prigogine-Lefever mechanism at a single active site in an infinite medium. Shymko and Glass[7] investigated the number and stability of steady states of a two-site problem in which nonlinear activation and inhibition is described by the so-called Hill function. Bimpong-Bota *et al.*[8] extended their earlier work to include periodic lattices of active sites.

In this section we describe a novel procedure that uses conformal mapping to determine sufficient conditions for linear stability of a steady state. In situations in which the technique can be applied, the complex problem of determining conditions under which the roots of a transcendental equation lie in the region $\mathrm{Re}(s)<0$ reduces to determining conditions under which a polynomial equation has roots in a transformed stability region. In addition to being able to derive stability criteria for given situations, the technique provides useful insight into the way in which the various physical processes influence stability by altering the shape and extent of the transformed stability region.

We introduce the procedure by way of some simple examples and discuss the manifestation of the various physical processes in the deformation of the stability regions.

A. Steady-state solutions

The equations governing the steady-state solutions of the diffusion-localized-reaction system (2.1) are obtained by setting $\partial \mathbf{u}/\partial t = 0$. In the examples that follow, we consider a single active site at $x=0$ in a domain $[-L,L]$ so that (2.1) reduces to the system

$$D_i u_i - \Omega_i u_i + f_i = 0$$

$$\text{with } i=1,2,\ldots,S \text{ for } x\in(-L,L)\ , \tag{3.1a}$$

$$-D_i[u_i']_{x=0} = R_i(u_j(0))\ . \tag{3.1b}$$

A further assumption we make in what follows is that $f_i(x)=\text{const}$ and $g_{ir}=\text{const}$ in (2.2b).

We now consider a variety of boundary conditions.

(i) Homogeneous Dirichlet boundary conditions ($\underline{\alpha}_r=\underline{0}$, $\underline{\beta}_r\neq\underline{0}$, $\mathbf{g}_r=0$; $r=0,N$). In this case, the solution to (3.1) is given by

$$u_i(x)=u_i(0)\frac{\sinh[\omega_i(L-|x|)]}{\sinh(\omega_i L)}+\frac{f_i}{\Omega_i}\left[1-\frac{\sinh[\omega_i(L-|x|)]+\sinh(\omega_i|x|)}{\sinh(\omega_i L)}\right], \tag{3.2a}$$

where $\omega_i=(\Omega_i/D_i)^{1/2}$ and $u_i(0)$ is the solution of the system of nonlinear equations

$$2D_i\omega_i\coth(\omega_i L)[u_i(0)+F_i]=R_i(u_j(0))\ , \tag{3.2b}$$

arising from (3.1b) and where

$$F_i=\frac{f_i}{\Omega_i}\left[\frac{1-\cosh(\omega_i L)}{\sinh(\omega_i L)}\right].$$

(ii) Homogeneous Neumann boundary conditions ($\underline{\alpha}_r\neq\underline{0}$, $\underline{\beta}_r=\underline{0}$, $\mathbf{g}_r=0$; $r=0,N$). In this case, the solution to (3.1) is given by

$$u_i(x)=u_i(0)\frac{\cosh[\omega_i(L-|x|)]}{\cosh(\omega_i L)}+\frac{f_i}{\Omega_i}\left[1-\frac{\cosh[\omega_i(L-|x|)]}{\cosh(\omega_i L)}\right], \tag{3.3a}$$

where $u_i(0)$ is the solution of the system of nonlinear equations

$$2D_i\omega_i \tanh(\omega_i L)\left[u_i(0)-\frac{f_i}{\Omega_i}\right]=R_i(u_j(0)) \ . \quad (3.3b)$$

In the limit $L\to\infty$ both (3.2) and (3.3) reduce to

$$u_i(x)=u_i(0)e^{-\omega_i|x|}+\frac{f_i}{\Omega_i}(1-e^{-\omega_i|x|}) \ , \quad (3.4a)$$

where now $u_i(0)$ is the solution of the system of nonlinear equations

$$2D_i\omega_i(u_i(0)-f_i/\Omega_i)=R_i(u_j(0)) \ . \quad (3.4b)$$

It is interesting to contrast the nature of the steady-state solutions to the diffusion-localized-reaction equations with those of the system of ordinary differential equations having the same reaction term, i.e.,

$$\dot{u}_i=R_i(u_j) \ . \quad (3.5a)$$

In this case, the steady states are given by the solutions to the system of nonlinear equations

$$0=R_i(u_j) \ . \quad (3.5b)$$

Comparing (3.5b) with (3.2b), (3.3b), and (3.4b), we notice that the diffusing bulk only introduces at most linear terms to (3.5b). In fact, if we restrict ourselves to bimolecular mechanisms such as those considered by Tyson and Light,[15] then it can be seen from the detailed signs of the linear terms introduced by the diffusing bulk that just as wide a variety of steady states are admitted by both systems. For a given reaction term $R_i(u_j)$ the presence of the diffusing-desorbing bulk can change the regime of a reaction from a single steady state in the ordinary differential equation (ODE) case to multiple steady states in the active site case. In fact, as the parameters D_i, Ω_i, and L are varied, the number of steady states can change. This has been demonstrated by Shymko and Glass[7] and Bimpong-Bota *et al.*[6,8]

B. Linear stability analysis

Let $u_i^*(x)$ be a steady solution of (2.1). We consider a small perturbation $V_i^0(x)$ to the steady state $u_i^*(x)$ and let $V_i(x,t)$ be the subsequent evolution of this initial perturbation. The equation governing the evolution of $V_i(x,t)$ can be obtained by perturbation of (2.1):

$$\frac{\partial V_i}{\partial t}=D_i\frac{\partial^2 V_i}{\partial x^2}-\Omega_i V_i+\sum_{l=1}^{L}\sum_{j=1}^{S}J_{ij}(u_k^*(x_l))V_j\delta(x-x_l) \ , \quad i=1,2,\ldots,S \quad (3.6a)$$

where $J_{ij}(u_k)=\partial R_i/\partial u_j(u_k)$. The perturbed boundary conditions are obtained from (2.2b):

$$\left[\alpha_{i,r}\frac{\partial}{\partial x}+\beta_{i,r}\right]V_i(x_r,t)=0, \quad r=0,N \ . \quad (3.6b)$$

We use Laplace transforms to analyze the growth or decay of the perturbation $V_i(x,t)$. Taking the Laplace transform of (3.6) and using the jump conditions (2.3), we obtain

$$\bar{V}_i''(x,s)-\omega_i^2(s)\bar{V}_i(x,s)=-\frac{V_i^0(x)}{D_i}, \quad i=1,2,\ldots,S \quad (3.7a)$$

$$-D_i[\bar{V}_i'(x,s)]_{x=x_l}=\sum_{j=1}^{S}J_{ij}(u_k^*(x_l))\bar{V}_j(x_l,s) \ , \quad (3.7b)$$

$$\left[\alpha_{i,r}\frac{\partial}{\partial x}+\beta_{i,r}\right]\bar{V}_i(x_r,s)=0 \ , \quad (3.7c)$$

where $\omega_i(s)=[(s+\Omega_i)/D_i]^{1/2}$ and the prime denotes $\partial/\partial x$. In order to simplify the analysis we return to the problem of a single active site at $x=0$ in a domain $[-L,L]$, which was introduced in Sec. III A, and assume that the initial perturbation $V_i^0(x)$ is constant.

The solution $\bar{V}_i(x,s)$ of (3.7) is then given by (3.2a), (3.3a), and (3.4a) in which $u_i(x)$ is replaced by $\bar{V}_i(x,s)$, ω_i by $\omega_i(s)$, Ω_i by $(s+\Omega_i)$, and f_i by V_i^0. The solutions $\bar{V}_i(0,s)$ at the active site in each of the three cases are obtained by solving the following equations:

$$\sum_{j=1}^{S}[\psi_i(s)\delta_{ij}-J_{ij}(u_k^*(0))]\bar{V}_j(0,s)=F_i(s) \ ,$$

where we have the following for the various cases.

(i) Homogeneous Dirichlet boundary conditions:

$$\psi_i(s)=2D_i\omega_i(s)\coth[\omega_i(s)L] \ , \quad (3.8a)$$

$$F_i(s)=2V_i^0\left[\frac{\cosh[\omega_i(s)L]-1}{\omega_i(s)\sinh[\omega_i(s)L]}\right] \ . \quad (3.8b)$$

(ii) Homogeneous Neumann boundary conditions:

$$\psi_i(s)=2D_i\omega_i(s)\tanh[\omega_i(s)L] \ , \quad (3.9a)$$

$$F_i(s)=2V_i^0\frac{\tanh[\omega_i(s)L]}{\omega_i(s)} \ . \quad (3.9b)$$

(iii) $L\to\infty$ with either boundary condition:

$$\psi_i(s)=2D_i\omega_i(s) \ , \quad (3.10a)$$

$$F_i(s)=\frac{2V_i^0}{\omega_i(s)} \ . \quad (3.10b)$$

We apply the Laplace transform inversion theorem[16] to $\bar{V}_i(x,s)$. Firstly we note that the singularities of $V_i(x,s)$ that are due to the localized reaction are given by the condition

$$\det[\psi_i(s)\delta_{ij}-J_{ij}]=0 \ . \quad (3.11)$$

Next we observe that $F_i(s)$ in (3.8) and (3.9) has removable singularities at $s=-\Omega_i$; $F_i(s)$ in (3.10) has a branch point singularity at $s=-\Omega_i$, which gives rise to a contribution that decays as $e^{-\Omega_i t}/t^{3/2}$ as $t\to\infty$; and the only other remaining singularity of $\bar{V}_i(x,s)$ is a simple pole at $s=-\Omega_i$. Therefore, we conclude that the contributions of the singularities due to the linear bulk all decay as $t\to\infty$ provided $\Omega_i>0$. This is to be expected as we are

considering a stable linear bulk. Thus the only instabilities that can arise are those from the roots of the determinantal condition (3.11).

It should be noted that $\psi_i(s)$ in (3.10a) is the stability function used by Bimpong-Bota *et al.*[6] to analyze the stability of a single active site in an infinite domain. Moreover, the function $\psi_i(s)$ in (3.8a) is that used by Bimpong-Bota *et al.*[8] to analyze the stability of a periodic lattice. We shall refer to these stability functions $\psi_i(s)$ as "domain functions" as they represent the geometry and material properties of the linear bulk.

C. Conformal mapping of the stability region $\mathrm{Re}(s)\leq 0$ by the domain functions $\psi_i(s)$

First, for simplicity, we assume some linear relationship between the $\psi_i(s)$. For example, $\psi_1(s)=\cdots=\psi_S(s)=\psi(s)$, which applies in the case of equal diffusion and desorption. In this case, (3.11) reduces to determining the roots of an Sth-degree polynomial $P_S(\psi^*)=0$ which is determined by the reaction process taking place at the defects. We now consider the image of the stability region $\mathrm{Re}(s)\leq 0$ under the map $w=\psi(s)$. This interpretation of (3.11) essentially decouples the bulk diffusion-desorption processes from the defect reaction processes. The mapped stability regions associated with (3.8a), (3.9a), and (3.10a) are plotted in Figs. 1(a), 1(b), and 1(c), respectively. In all the plots presented in Fig. 1 we assume $D=1.0$.

In Fig. 1(a) the stability regions for the homogeneous Dirichlet boundary-condition problem (3.8) are plotted for various interval lengths $L=1,2,4$ with desorption ($\Omega=2$) and without desorption (i.e., $\Omega=0$). The curves plotted are the images of the imaginary s axis: $x=ia$ where $a\in\mathbb{R}$. These curves $C(L,\Omega)$ form the rightmost boundary of the stability region. Thus a root ψ^* of the polynomial equation $P_S(\psi^*)=0$ is stable, provided it lies to the left of the applicable curve $C(L,\Omega)$. It is interesting to note, by comparing the curves $C(L,0)$ with those of $C(L,2)$, that desorption increases the extent of the stability region. This is consistent with physical intuition. As an example of the way in which the stability regions can be used to derive stability criteria, assume that the roots ψ^* of the polynomial equation $P_S(\psi^*)=0$ are all real and let $\psi^*_{\max}$ denote the maximum root. Then since the intercept of the axis $\mathrm{Im}(w)=0$ and the stability curves in this case are given by

$$w=\frac{2D}{L}\left[\left(\frac{\Omega}{D}\right)^{1/2}L\right]\coth\left[\left(\frac{\Omega}{D}\right)^{1/2}L\right]$$

$$\rightarrow\frac{2D}{L}\quad\text{as }\Omega\rightarrow 0\,,$$

we immediately obtain the stability criterion

$$\psi^*_{\max}\leq\frac{2D}{L}\left[\left(\frac{\Omega}{D}\right)^{1/2}L\right]\coth\left[\left(\frac{\Omega}{D}\right)^{1/2}L\right]. \tag{3.12a}$$

It is interesting to note that in the absence of desorption the stability criterion reduces to

$$\psi^*_{\max}\leq\frac{2D}{L}\,. \tag{3.12b}$$

This reflects the stabilizing effect of the Dirichlet boundary conditions that allow material to escape at the boundaries. The criterion (3.12b) is a statement of the fact that the characteristic diffusion velocity for the interval should be larger than the maximum velocity of material produced by the localized reaction at $x=0$. From Fig. 1(a) it can be seen that the stability introduced by escape of material at the boundaries decreases as the length L of the interval increases. In addition, when desorption is present, the stabilizing effect of the escape of material at the boundaries is subdominant to that of desorption.

In Fig. 1(b) the stability regions are provided for the case of Neumann boundary conditions (3.9) with the same range of values of interval length L and desorption Ω as in Fig. 1(a). Again the stabilizing effect of desorption can be seen clearly by comparing $C(L,0)$ with $C(L,2)$. In this figure it can be seen that the effect of the Neumann boundary condition is quite different from that of the Dirichlet boundary condition shown in Fig. 1(a). Since no material can escape at the boundaries, we see that any positive real roots ψ^* of $P_S(\psi^*)=0$ are unstable in the absence of desorption. As the interval length L is decreased, the stability region is seen to shrink in each case. Since these boundary conditions effectively embed the defect in a periodic lattice of defects with spacing $2L$, we see that decreasing the interdefect spacing $2L$ has a cooperative destabilizing effect. If we assume (as was done with the previous case) that $P_S(\psi)$ has only real roots, we obtain the stability criterion

$$\psi^*_{\max}\leq\frac{2D}{L}\left[\left(\frac{\Omega}{D}\right)^{1/2}L\right]\tanh\left[\left(\frac{\Omega}{D}\right)^{1/2}L\right]. \tag{3.13}$$

This criterion will be used in Sec. IV to analyze reactive trapping by defects on a catalytic surface.

In Fig. 1(c) the stability regions are provided for the infinite domain limit $L\rightarrow\infty$ of the above two cases for various values of desorption Ω. The increase of the extent of the stability regions with desorption can be clearly observed. The stability boundary in the case $\Omega=2$ and $L\rightarrow\infty$ shown in Fig. 1(c) agrees well with that of Figs. 1(a) and 1(b) with $\Omega=2$ and only modestly large values of $L=2,4$. It is interesting to note that the infinite domain, in spite of its capacity to accept material, will not be stable without desorption if $P_S(\psi)$ has any positive real roots. If we again assume $P_S(\psi)$ has only real roots, then we obtain the stability criterion

$$\psi^*_{\max}\leq 2\sqrt{D\Omega}\,. \tag{3.14}$$

This is a statement of the fact that the characteristic desorption velocity should be larger than the maximum velocity of material produced by the localized reaction at $x=0$. From (3.14) it can be seen that the stabilizing effect of the desorption relies on the diffusion process to spread the material before it can be desorbed.

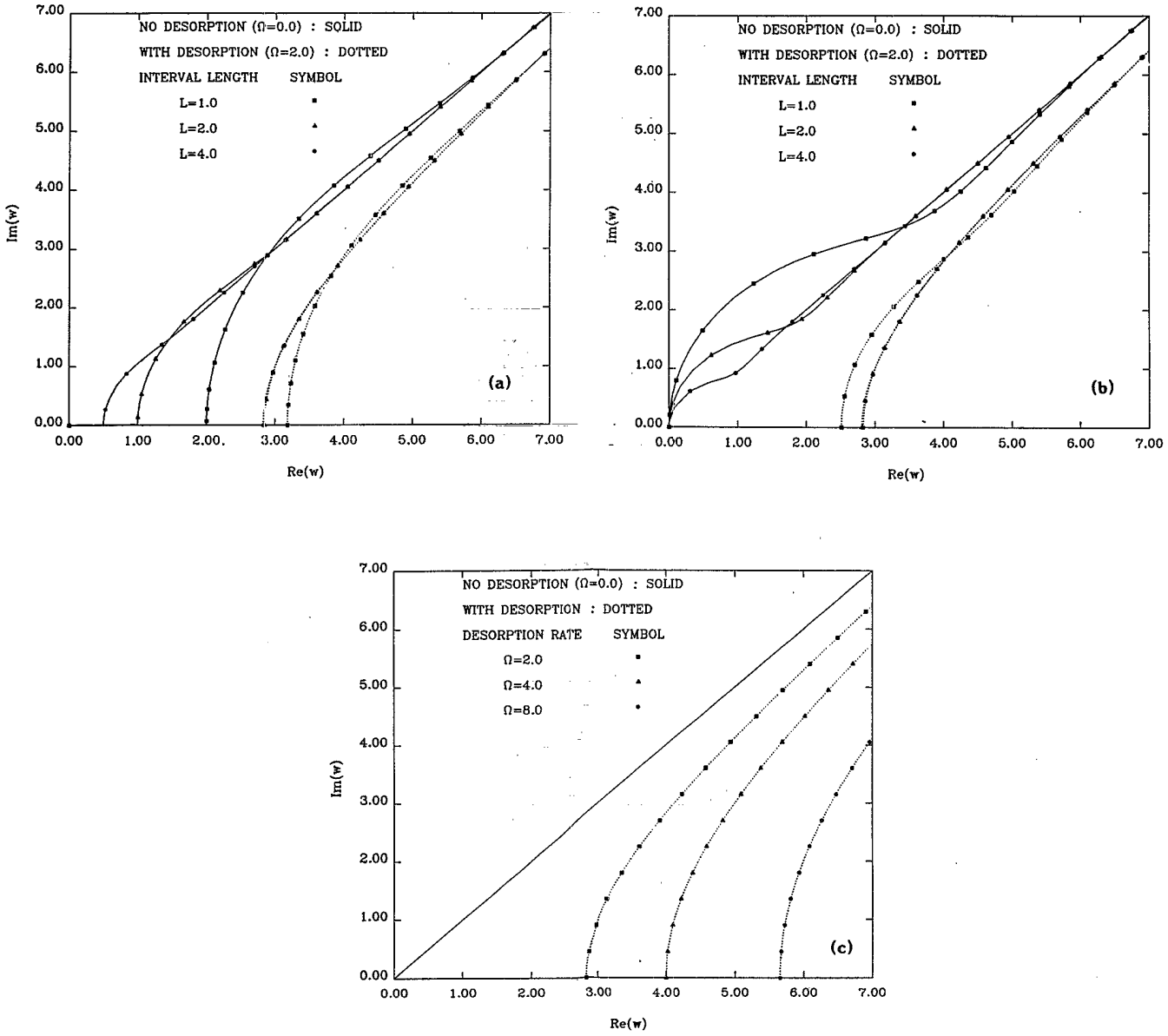

FIG. 1. (a) The mapped stability region associated with the homogeneous Dirichlet boundary-condition problem (3.2) with the domain function defined in (3.8). The curves $C(L,\Omega)$ shown for the different parameter values represent the right-most boundary of the stability region so that the stability region lies to the left of these curves in each case. In these cases it can be seen that as L, the length of the interval, decreases the stability region grows. This is due to the stabilizing effect of the homogeneous Dirichlet boundary conditions which allow material to escape from the boundaries. The stabilizing effect of desorption can be seen by comparing the solid curves $C(L,0)$ with the corresponding dotted curves $C(L,2)$. When $\Omega\neq 0$ the stabilizing effect of the escape of material from the boundaries is subdominant to the stability provided by desorption, as can be seen by comparing $C(2,2)$ with $C(4,2)$. In order to establish a stability criterion in a given situation, we need only ensure that the roots of the polynomial equation $P_S(\psi^*)=0$ lie to the left of the applicable curve. (b) The mapped stability regions associated with the homogeneous Neumann boundary-condition problem (3.3) with the domain function defined in (3.9). The stabilizing effect of desorption can be seen clearly by comparing $C(L,0)$ with $C(L,2)$. The role of L, however, is quite different in this situation. A decrease in L in this case has the effect of reducing the extent of the stability region. Since the boundary conditions effectively embed the defect in a periodic lattice of defects, decreasing L decreases the interdefect spacing, which has a cooperative destabilizing effect. Again, the stability criteria can be obtained in a given situation by requiring that the roots of $P_S(\psi^*)=0$ lie to the left of the applicable stability curve. (c) A single defect in an infinite domain $L\rightarrow\infty$. The increase of the stability boundary with desorption can be clearly observed. The stability boundary in the case $\Omega=2$ shown here agrees well with that of only modestly large values of $L=2$ and 4 shown in (a) and (b). We observe that an infinite domain in spite of its capacity to accept material will not be stable if $P_S(\psi)$ has any positive real roots. As before, stability criteria can be obtained in a given situation by requiring that all the roots of $P_S(\psi^*)=0$ lie to the left of the applicable curve.

D. Comments

We have introduced the concepts of multiple steady states and stability, which will be used later in the paper. We have also outlined a novel procedure that uses conformal mapping to gain insight into the way in which various physical processes influence stability. Using this approach it is possible to derive criteria for stability by merely determining conditions under which a polynomial equation will have roots in a transformed stability region. We have derived stability criteria that will be used later in the context of reactive trapping by defects on a catalytic surface.

The conformal mapping technique outlined in this section can also be used to analyze the stability of diffusion-localized-reaction problems in dimensions greater than one. In this case, the domain functions $\psi_i(s)$ will be expressed in terms of eigenfunctions of the Laplacian operator for the geometry of the defect surface. For example, an infinitely long cylindrical defect with radius a has a domain function

$$\psi_i(s)=\frac{D_i\omega_i(s)I_0'(\omega_i(s)a)}{I_0(\omega_i(s)a)} ,$$

where I_0 is the zeroth-order modified Bessel function of the first kind. Since the analysis that follows is essentially restricted to one-dimensional problems we do not pursue the higher-dimensional stability analysis here.

IV. REACTIVE TRAPPING BY DEFECTS: THE CONTINUUM ASSUMPTION AND THE EFFECT OF SMALL SYMMETRY-BREAKING PERTURBATIONS ON DESORPTION PROCESSES

In this section we analyze the effect of defects on desorption from a catalytic surface using the continuum model (2.1). The continuum model should provide a good approximation to the physical situation when the number of atoms between the defects becomes large. We shall validate this statement. This one-dimensional model represents a lattice of parallel line or step defects on the surface. We shall assume that a process of reactive trapping at defects occurs in which the defects act as sinks of material that ultimately desorbs as a product. We investigate the effect of the distribution of defects on the balance between the bulk desorption and the desorptive process taking place at the defects themselves.

A. Validation of the continuum approximation

In this section we consider a discrete physical system comprising $m+1$ sites. The site with index 0 is assumed to be a defect site at which reactive trapping occurs. Material passes between neighboring sites on the surface by a diffusion process with rate constant k_H. Material is desorbed from each site in proportion to the fractional occupation η_i at the site with a rate constant k_T. Material is also adsorbed at each site at a rate I. At the defect site, material is trapped with a rate coefficient $-k_S(1-\gamma\eta_0)$, where η_0 is the fractional occupation at the defect. The decrease of this rate coefficient with increasing η_0 incorporates an access limitation or saturation process at the defect. The equations governing all these processes are as follows:

$$\dot{\eta}_i=k_H\Delta^2\eta_{i-i}-k_T\eta_i+I-k_S(1-\gamma\eta_i)\eta_i\delta_{i,0} , \qquad i=0,1,\ldots,m \quad (4.1a)$$

$$\delta\eta_m=0, \quad \eta_{-1}=\eta_1 . \quad (4.1b)$$

Here Δ is the forward difference operator defined by $\Delta\eta_i=\eta_{i+1}-\eta_i$, δ is the central difference operator defined by $\delta\eta_i=\eta_{i+1}-\eta_{i-1}$, $\delta_{i,j}$ is the Kronecker delta defined by $\delta_{i,j}=0$ if $i\neq j$ and 1 if $i=j$, and η_i is the fractional occupation. We notice from the boundary conditions (4.1b) that Eqs. (4.1) determine the fractional occupation of a typical defect in a periodic array of defects. By symmetry only half of the interval between any two defects is considered.

Physically, the reactive-trapping process taking place at the defect sites may represent the conversion at the defects of the species under consideration to a different species. The product species may be less important to the reaction-diffusion process taking place on the surface, or may be used by another reaction process that is decoupled from the original species other than through the sources of the product species provided by the defects. In the latter case, saturation of the defect site will occur if the product species is formed at a rate larger than the rate at which it is removed by the secondary decoupled reaction system. Equations (4.1) are formally similar to those used by Serri *et al.*[1] to model the effects of steps on desorption of NO from a Pt(111) surface. Their model differed from (4.1) in that the nonlinear term was located at two different points and represented accumulation of material at a step owing to a difference between the incoming and outgoing diffusion rate constants. The process of reactive trapping being considered in (4.1) is physically quite different from that of diffusion-based accumulation.

In order to obtain a continuum approximation for the above reactive-trapping model, we assume that $m\to\infty$ and h, the distance between sites on the surface, approaches zero in such a way that $mh=L=$const. In this limit we obtain

$$\frac{\partial u}{\partial t}=D\frac{\partial^2 u}{\partial x^2}-\Omega u+f-R_S(1-\bar{\gamma}u)u\,\delta(x) , \quad (4.2a)$$

where $D=h^2k_H$, $\Omega=k_T$, $f=I/h$, $R_S=hk_S$, $\bar{\gamma}=h\gamma$, and $u(x)=\lim_{h\to 0}(\eta_i/h)$ is now the concentration of material at the point x. The appropriate boundary conditions for this problem are

$$\frac{\partial u}{\partial x}(x=\pm L,t)=0 . \quad (4.2b)$$

The steady-state solution for (4.2) is given by (3.3a) in which the subscripts are dropped since we are only considering one species. The solutions to (3.3b) in this case are

$$u^{\pm}(0)=\frac{B\pm(B^2-4Ac)^{1/2}}{2A} , \quad (4.3)$$

where

$$A=\bar{\gamma}R_S ,$$

$$B=R_S+2D\omega\tanh(\omega L) ,$$

$$C=2f\tanh(\omega L)/\omega .$$

In order to analyze the stability of these solutions, we use the determinantal condition (3.11), which is this case reduces to

$$\psi^*(s)=R_S(1-2\bar{\gamma}u(0)) . \tag{4.4}$$

Combining (4.3) with (4.4) we can show that if the roots $u^{\pm}(0)$ are real, then the stability criterion (3.13) is satisfied by the negative branch of (4.3), while the positive branch is always unstable. If the roots have imaginary parts, the rate of adsorption f is so large that no equilibrium level due to trapping by the defect can exist. This is beyond the regime of defect trapping in which we are interested.

In Fig. 2 we plot the steady-state concentration for a number of discrete systems (4.1) having different numbers of sites. Each of these discrete systems is approximated by the same continuum model. The solutions to the ordinary differential equations (4.1) of the discrete systems have been generated numerically using Gear's algorithm for solving nonlinear ODE's. We observe that there is a close correspondence between all the discrete and continuum models, which improves as the number of atoms in the discrete model is increased. We see that the continuum assumption is valid even when there are as few as $2m=20$ atoms between defects.

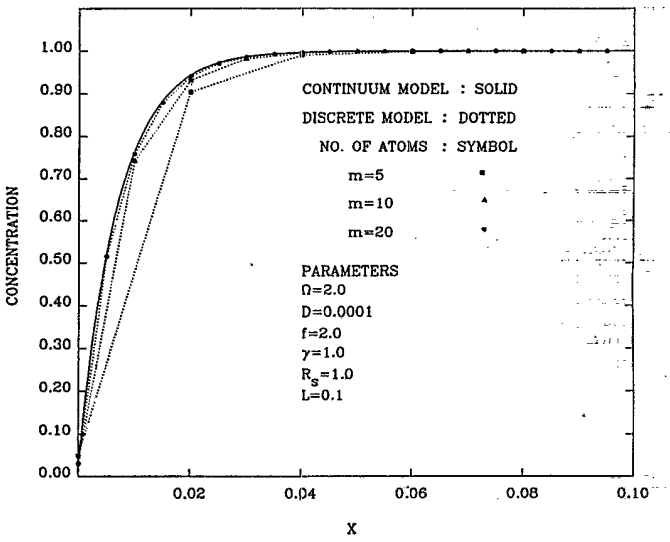

FIG. 2. The steady-state concentrations for discrete systems with reactive trapping at $x=0$, and having $2m=10,20,40$ interdefect sites, are compared with the continuum approximation to these systems. As expected, the continuum assumption improves as m increases. However, it is remarkable that the continuum approximation is this accurate for as few as 20 interdefect sites.

B. The effect of symmetry-breaking perturbations on desorption

In this section we consider the effect of symmetry-breaking perturbations to the defects upon the desorption processes on a surface with a nominal periodic array of defects. In the unperturbed case we assume that the defects are located at $x_n=n2L$ so the continuum model is of the form

$$\frac{\partial u}{\partial t}=D\frac{\partial^2 u}{\partial x^2}-\Omega u+f+\sum_{n=N}^{N}\delta(x-x_n)R(u(x)) , \tag{4.5a}$$

$$\frac{\partial u}{\partial x}(\pm r,t)=0 , \tag{4.5b}$$

$$u(x,0)=0 .$$

Here the reaction term $R(u)$, which is generally nonlinear, is assumed to provide a model for the trapping effect of the defects, the length of the domain is $2r=2LN$, and f is assumed to be constant.

The analysis we present here will be primarily concerned with reactive trapping at defects in which the defects act as sinks of material. The defects then act as localized regions of desorption of final product material. We shall distinguish between defect-based desorption and bulk desorption that occurs throughout the domain $[-r,r]$—as represented by the term $-\Omega u$ in (4.5a). The reason for this distinction is that we may wish to consider reactive trapping at defects in which the species under consideration is converted at the defect to a different species. This product species may be less important to the reaction diffusion process taking place on the surface and may, therefore, be regarded as removed from the system. Observations of material desorbed from the surface (i.e., $-\Omega\int_{-r}^{r}u\,dx$) in this case will not detect the product species although material has effectively been lost by the system. Another situation that can arise is that the species produced at the defects enters into another reactive process decoupled from the original species. In this case the balance between the defect desorption and the bulk desorption becomes extremely important.

Since the material is conserved, the steady-state *total* desorption rate is just f—the rate of adsorption of material to the surface (assuming the reaction causes no net change in the total moles of all species together). Therefore, the interesting quantity in the above situation is not the total desorption rate, but the subdivision of the desorption between the two desorptive processes described above. To avoid confusion in the following analysis, we refer to the bulk desorption process as the desorption; the defect desorption process is referred to as reactive trapping. Therefore, the average desorption rate over the interval $[-r,r]$ is defined to be

$$\mathcal{D}=\frac{1}{2r}\int_{-r}^{r}\Omega u\,dx . \tag{4.6}$$

A convenient expression for the average steady-state desorption rate over the interval $[-r,r]$ can be obtained by integrating (4.5) with $\partial u/\partial t=0$ to obtain

$$\mathcal{D}=\frac{1}{2r}D\frac{\partial u}{\partial x}\Bigg|_{-r}^{r}+f+\frac{1}{2r}\sum_{n=-N}^{N}R(u(x_n))$$

$$=f+\frac{1}{2r}\sum_{n=-N}^{N}R(u(x_n)) \tag{4.7}$$

using (4.5b).

For the purposes of the analysis that follows, we shall place only a few restrictions on the form of the function $R(u)$ so as to admit a wide class of reactive-trapping models. We shall assume that the domain of interest is $[0,u_S]$ and that $R(u)$ has the following properties:

(R1) $R(u)$ is analytic on $[0,u_S]$.

(R2) $R(0)=0$. This ensures that if there is no material on the surface, then no reactive trapping can take place at the defects.

(R3) $R(u)<0$ for $u\in(0,u_S)$. Since R is negative on the domain of interest the defects act as sinks of material.

(R4) There exists a critical point $u_C\in(0,u_S)$ for which $R'(u_C)=0$.

For $u\in[0,u_C)$ we assume $R'(u)<0$. In this interval an increase in the concentration u at the defect causes an increase in the magnitude of the sink.

For $u\in(u_C,u_S]$ we assume $R'(u)>0$. Within this interval, an increase in the concentration u at the defect causes a decrease in the magnitude of the sink. Physically, this represents a process of saturation or crowding at the defect, which limits access to the defect. We assume that $R(u_S)=0$ so that the defect is eventually rendered inoperative when the concentration at the defect reaches a certain level. This access limitation mode can also be interpreted as a saturation of the defect by the product species in the reactive-trapping process. This will occur if, for example, the rate at which the product species is deposited is larger than the rate at which it is used by the secondary decoupled reaction system.

(R5) $R''(u)>0$ for $u\in[0,u_S]$. This assumption restricts the model to a single critical point u_C. The possibility of multiple critical points is not excluded by the formal analysis that follows, but is excluded to simplify the interpretation of the results.

Assumption (R1) is formally fundamental to the analysis that follows. Assumptions (R2) and (R3) ensure that the defects represent reactive trapping of material. The importance of (R4) is to include in the model a region of enhanced trapping with increased defect concentration followed by a region of access limitation or saturation when the defect concentration is increased above a certain level. Assumption (R5) should be excluded if multiple critical points are to be considered. The analysis that follows applies to a wide class of reactive-trapping models that satisfy conditions (R1)–(R5). In order to illustrate this analysis, we shall make use of the following simple model:

$$R(u)=-(1-\gamma u)u\ . \tag{4.8}$$

$R(u)$ defined in (4.8) can be seen to satisfy conditions (R1)–(R5) in which $u_C=1/2\gamma$ and $u_S=1/\gamma$.

1. The case of a single active site

It is illustrative to consider a symmetry-breaking perturbation to a single defect at $x=0$, which is initially at the midpoint of the domain, to a new position $x=\varepsilon$. In this case the solution is governed by (4.5) in which $N=0$ and $r=L$. This situation is of interest since it provides a special case of (4.5) in which the effect of a symmetry-breaking perturbation can be solved analytically. Moreover, if one were to assume that the effect of perturbing one defect in (4.5) were so localized that even the nearest neighbors were not influenced, then this simplified system would provide an approximation to the case of the full periodic array. We shall see that this simplified problem does indeed exhibit similar behavior to that of the periodic lattice and provides a useful frame of reference to separate effects of the periodic lattice from those that are essentially local. We illustrate this special case using the reactive-trapping model (4.8). However, the expressions for the solution and the perturbed desorption rate are provided in a form that applies to any defect trapping model.

The solution to (4.5) with $N=0$, and $r=L$, is given by

$$u_\varepsilon(x)=\begin{cases}\dfrac{f}{\Omega}-\left[\dfrac{f}{\Omega}-u_\varepsilon(\varepsilon)\right]\dfrac{\cosh[\omega(L+x)]}{\cosh[\omega(L+\varepsilon)]}, & x<\varepsilon\\[2ex] \dfrac{f}{\omega}-\left[\dfrac{f}{\Omega}-u_\varepsilon(\varepsilon)\right]\dfrac{\cosh[\omega(L-x)]}{\cosh[\omega(L-\varepsilon)]}, & x>\varepsilon\end{cases} \tag{4.9a}$$

where $\omega=(\Omega/D)^{1/2}$. In the case of the reactive-trapping model (4.8), $u_\varepsilon(\varepsilon)$ is given by

$$u_\varepsilon^{\pm}(\varepsilon)=\frac{(T+1)\pm[(T+1)^2-4f\gamma T/\Omega]^{1/2}}{2\gamma}\ , \tag{4.9b}$$

where $T=\{\tanh[\omega(L+\varepsilon)]+\tanh[\omega(L-\varepsilon)]\}\omega D$. It should be noted that when $\varepsilon=0$ the perturbed solution (4.9) reduces to the unperturbed solution given in (3.3). The unperturbed ($\varepsilon=0$) and perturbed ($\varepsilon>0$) solutions (4.9) for two different interval widths L are plotted in Figs. 3(a) and 3(b). The parameters used in these two cases were $\Omega=2.0$, $D=1.0$, $f=2.0$, $\varepsilon=0.02$, and $\gamma=1.0$; while the interval widths were $L=0.1$ and 0.2 in Figs. 3(a) and 3(b), respectively.

Combining the determinantal condition (3.11) with the stability criterion (3.13) we obtain the following stability condition for the unperturbed solution $u_0(x)$:

$$R'(u_0(0))<2\omega D\tanh(\omega L)\ . \tag{4.10a}$$

When R is given by (4.8),

$$-1+2\gamma u_0(0)<2\omega D\tanh(\omega L)\ . \tag{4.10b}$$

Making use of (4.9b) with $\varepsilon=0$ it is possible to show that if the roots are real, then the negative branch given in (4.9b) is always stable. The situation of imaginary roots corresponds to the input function f being so large that no equilibrium level due the defect can exist. In this case an equilibrium concentration f/Ω will be achieved, which represents a balance between adsorption and desorption as if no defect were present. Since we are interested in

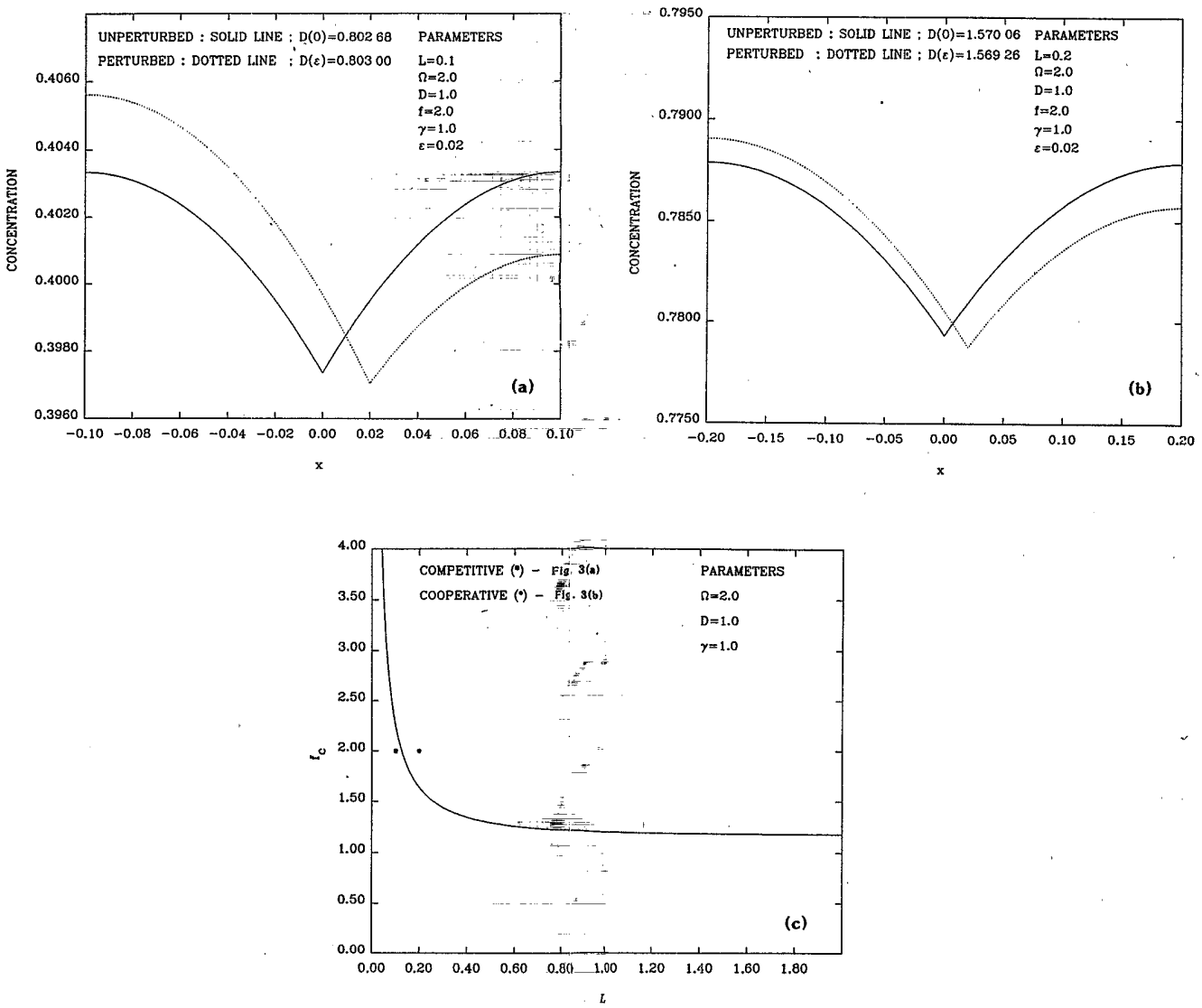

FIG. 3. (a) The unperturbed and perturbed concentration profiles for the case of a single defect are plotted. The single defect may be regarded as embedded in a periodic array of defects. The perturbation for this parameter set causes the defect to *compete* with its closer neighbor for material to trap. This causes the desorption rate $\mathcal{D}(\varepsilon)$ to be *larger* than the unperturbed desorption rate $\mathcal{D}(0)$. (b) The unperturbed and perturbed concentration profiles for the case of a single defect are plotted. Again we regard the single defect to be embedded in a periodic array of defects. The perturbation for this parameter set causes the defect to *cooperate* with its closer neighbor to reduce the local saturation level. This in turn causes the desorption rate $\mathcal{D}(\varepsilon)$ to be *smaller* than the unperturbed desorption rate $\mathcal{D}(0)$. (c) The critical adsorption level f_c is plotted as a function of L, the half-spacing between defects. To the left of or below this curve the defects will act in a competitive fashion when perturbed and the perturbed desorption rate $\mathcal{D}(\varepsilon)$ will be larger than the unperturbed desorption rate $\mathcal{D}(0)$. Above and to the right of this curve, cooperative behavior prevails. It can be seen that for any adsorption level, it is always possible to achieve competitive behavior by decreasing the interdefect spacing $2L$. This is due to the strong interaction between defects that are close together. The asymptote $L \to \infty$ in this figure corresponds to weak interaction between neighboring defects.

equilibria related to trapping by the defect, this level of adsorption is beyond that in which we are interested.

Both the unperturbed solutions shown in Fig. 3 are stable. In the case of the shorter interval $L=0.1$ [shown in Fig. 3(a)] the unperturbed defect concentration is $u_0(0)=0.3974$. Perturbation reduces the defect concentration to $u_\varepsilon(\varepsilon)=0.3970$. The desorption rate in the unperturbed case is $\mathcal{D}(0)=0.802\,68$, while in the perturbed case the desorption rate *increases* to $\mathcal{D}(\varepsilon)=0.803\,00$. In the case of the larger interval $L=0.2$ [shown in Fig. 3(b)], the unperturbed defect concentration is $u_0(0)=0.779\,32$, while in the perturbed case the defect concentration is reduced to $u_\varepsilon(\varepsilon)=0.778\,75$. The situation for the desorption rate, however, is quite different. The unperturbed desorption rate is $\mathcal{D}(0)=1.570\,06$, whereas perturbation *decreases* the desorption rate to $\mathcal{D}(\varepsilon)=1.569\,26$.

In order to explain this phenomenon, we determine the

parameters that govern the perturbed desorption rate by expanding $\mathcal{D}(\varepsilon)$ in powers of ε. Applying the perturbation procedure that will be outlined in the next section, we obtain the following expansion for the perturbed desorption rate $\mathcal{D}$:

$$\mathcal{D}(\varepsilon)=\mathcal{D}_0+\varepsilon^2\mathcal{D}_2+\cdots,$$

where $\mathcal{D}_0$ is the unperturbed desorption rate and

$$\mathcal{D}_2=R'(u_0(0))\left[\frac{D\{[u_1''(0)]+\frac{1}{2}[u_0'''(0)]\}+2D\omega\tanh(\omega L)\{u_1'(0)+\frac{1}{2}u_0''(0)\}}{2D\omega\tanh(\omega L)-R'(u_0(0))}\right]. \tag{4.11a}$$

Here [ ] denotes the jump-condition operator defined in (2.3); $u_1(x)$ is the first-order perturbation function that will be introduced in the next section; primes denote differentiation with respect to the appropriate arguments.

Making use of the differential equation (4.5a) (with $\partial u/\partial t=0$) and the jump conditions (2.3) it can be shown that (4.11a) can be expressed in the form

$$2r\mathcal{D}_2=\frac{R'(u_0(0))R(u_0(0))\omega^2[1-\tanh^2(\omega L)]}{2D\omega\tanh(\omega L)-R'(u_0(0))}. \tag{4.11b}$$

We assume that the perturbations are made to the stable steady states associated with reactive trapping by defects. Therefore, applying the stability criterion (4.10a), we observe that $2D\omega\tanh(\omega L)-R'(u_0(0))>0$. For reactive trapping by defects, (R3) implies that $R(u_0(0))<0$. It follows that the sign of the perturbation $\mathcal{D}_2$ to the desorption rate is determined by the sign of the gradient $R'(u_0(0))$ of the reaction term prevailing at the unperturbed defect. In particular, if $R'(u_0(0))<0$ then $\mathcal{D}_2>0$, whereas if $R'(u_0(0))>0$ then $\mathcal{D}_2<0$.

Two regimes of adsorption to the surface can thus be identified. In the case of the reactive-trapping model (4.8), the sign of $R'(u_0(0))$ is determined by the condition

$$\begin{aligned} f_C&=\frac{[4D\omega\tanh(\omega L)+1]\omega}{8\gamma\tanh(\omega L)}>f\Longleftrightarrow R'(u_0)<0\\ f_C&=\frac{[4D\omega\tanh(\omega L)+1]\omega}{8\gamma\tanh(\omega L)}<f\Longleftrightarrow R'(u_0)>0\,. \end{aligned} \tag{4.12}$$

Here f_C denotes the critical level of adsorption that separates the two regimes of adsorption. To interpret this condition physically, it is instructive to regard the single defect as embedded in a periodic lattice of defects. This assumption is valid in the unperturbed case $\varepsilon=0$, since the solutions for the periodic lattice and the unperturbed defect are identical due to the symmetry of the problem. We now assume that the perturbation of the defect does not appreciably affect the solution of the conceptual periodic lattice. In this case, within the interval $[-L,L]$ the solution to the perturbed lattice problem will be approximated by (4.9), and the perturbation to the desorption rate $\mathcal{D}_2$ will be approximated by (4.11b).

If $f<f_C$, $R'(u_0(0))<0$, then it follows from (4.11b) that the perturbation $\mathcal{D}_2$ to the desorption rate is positive. The physical interpretation of this result is that the perturbation causes the two defects in the lattice that are moved closer to compete for material to trap. This competitive behavior reduces the trapping efficiency of the lattice as a whole and the desorption rate increases. This situation corresponds to the solution for $L=0.1$ shown in Fig. 3(a), in which the concentration at the defect is decreased while the desorption rate is increased due to the perturbation.

If $f>f_C$, $R'(u_0(0))>0$, then it follows from (4.11b) that the perturbation $\mathcal{D}_2$ to the desorption rate is negative. The physical interpretation of this result is that the adsorption rate is sufficiently large that competition for material by the two closer defects no longer dominates the perturbation to the desorption rate. In fact, the influence of the two closer defects on the desorption rate is reversed. They now act in a cooperative fashion, each reducing the access limitation of the other by reducing the concentration locally. This situation prevails for the solution in Fig. 3(b) in which both the concentration at the defect decreased and the desorption rate decreased owing to the cooperative behavior of the closest defects.

It is interesting to note that the change of the direction in the condition (4.12) for the solutions given in Figs. 3(a) and 3(b) was achieved by increasing the lattice spacing from $L=0.1$ in 3(a) to $L=0.2$ in 3(b) rather than by varying the adsorption rate. This emphasizes that the regime of operation (either competitive or cooperative) is determined by a balance between the level of adsorption f and the other parameters such as the interdefect half-width L, the characteristic length scale of desorption $1/\omega$, and the access limitation or saturation parameter γ. As an illustration, the dependence of the critical adsorption level f_C on L is plotted in Fig. 3(c). In the region $L>1$, the defects are sufficiently far apart for the defects to act virtually independently. In this case f_C is insensitive to small changes in L. In addition, weak cooperative behavior can be expected for relatively modest values of adsorption, e.g., $f=1.5$. However, as $L\to 0$ the situation is reversed dramatically. In this case, defects interact in a highly competitive manner due to their close proximity, and will require high levels of adsorption f to supply enough material to the surface to move the defects into a cooperative regime. This high sensitivity of the critical adsorption level f_C to small changes in defect spacing emphasizes the enhanced effect defects have on one another when in close proximity. Without such an analysis, this complex behavior would be difficult to predict on the basis of physical intuition, especially in this complex nonlinear environment. For comparison, the level of operation of the two solutions plotted in Figs. 3(a) and 3(b) are also indicated in Fig. 3(c) by the solid square and circle, respectively.

We now comment on the above.

(1) It should be emphasized that the solution given in (4.9a) and the expression for the perturbation to the desorption given in (4.11a) apply for any analytic function $R(u)$ that is used to model the trapping effect of defects. The richness of information obtained using the simple model (4.8) of reactive trapping at defects emphasizes the usefulness of the continuum model (4.5) and the analytic tools that can be used to determine the structure of the solution.

(2) In the physical explanation for the phenomena observed, we assumed that the defect was embedded in a periodic lattice of defects and that the perturbation of the defect has little effect on the solution in the lattice and vice versa. In the next section we remove this assumption by performing a perturbation analysis in which the effects of the entire lattice are included. The effects due to the lattice defects away from the perturbed defect can then be identified clearly and contrasted with the single-defect case.

2. *Perturbation of a single defect in a periodic array of defects*

Readers more interested in the physical results may omit the mathematical development presented in this section and move to Sec. IV B 3 without a great loss of continuity.

Assume that the defect at $x_0=0$ in (4.5) is perturbed to $x_{0,\varepsilon}=\varepsilon$, while the remaining $2n$ defects remain at $x_n=2Ln$, $n=\pm1,\pm2,\ldots,\pm N$. We assume a two-sided perturbation expansion for the steady-state solution of (4.5), which is of the form

$$u_\varepsilon(x)=\begin{cases}u_0^-(x)+\varepsilon u_1^-(x)+\varepsilon^2u_2^-(x)+\cdots, & x<\varepsilon\\ u_0^+(x)+\varepsilon u_1^+(x)+\varepsilon^2u_2^+(x)+\cdots, & x>\varepsilon\end{cases}. \tag{4.13}$$

By allowing the freedom that results from the two-sided representation of $u_\varepsilon(x)$, it is possible to express the appropriate jump conditions at $x=\varepsilon$ in terms of jump conditions in the perturbation functions $u_i^\pm(x)$ around $x=0$. This subtle point is essential to be able to obtain the correct expansions of the solution in the vicinity of the singular points at which the derivative of the solution is discontinuous. This device also allows us to take advantage of the symmetry of the unperturbed lattice in order to eventually solve the perturbation equations order by order.

By requiring that $u_\varepsilon(x)$ be continuous at $x=\varepsilon$ in (4.13), by expanding the resulting condition about $x=0$ by Taylor's theorem, and by equating like powers in ε, we obtain the following conditions:

$$\begin{aligned}&\varepsilon^0>[u_0(0)]=0\,,\\ &\varepsilon^1>[u_0'(0)]+[u_1(0)]=0\,,\\ &\varepsilon^2>\tfrac{1}{2}[u_0''(0)]+[u_1'(0)]+[u_2(0)]=0\,,\\ &\cdots\,,\end{aligned} \tag{4.14}$$

where the operator $[\ ]$ is defined by $[u_K(0)]=u_K^+(0)-u_K^-(0)$, and the prime denotes differentiation with respect to x.

Combining the two-sided perturbation functions $u_i^\pm$ into a single function order by order, we see that (4.14) requires that $u_0(x)$ is continuous at $x=0$, while $u_1(x)$ has a jump at $x=0$, the magnitude of which is $-[u_0'(0)]$, and so on.

By the symmetry of the problem, the solutions for a positive ($\varepsilon>0$) and negative ($\varepsilon<0$) perturbation are related by

$$u_\varepsilon(-x)=u_{-\varepsilon}(x)\,. \tag{4.15}$$

We now decompose $u_\varepsilon(x)$ into symmetric and antisymmetric parts:

$$\begin{aligned}u_\varepsilon(x)&=u_\varepsilon^s(x)+u_\varepsilon^a(x)\\ &=\tfrac{1}{2}[u_\varepsilon(x)+u_\varepsilon(-x)]+\tfrac{1}{2}[u_\varepsilon(x)-u_\varepsilon(-x)]\\ &=\tfrac{1}{2}[u_\varepsilon(x)+u_{-\varepsilon}(x)]+\tfrac{1}{2}[u_\varepsilon(x)-u_{-\varepsilon}(x)]\end{aligned}$$

by use of (4.15). Therefore,

$$u_\varepsilon(x)=\begin{cases}u_0^-(x)+\varepsilon^2u_2^-(x)+\cdots+\varepsilon u_1^-(x)+\varepsilon^3u_3^-+\cdots, & \text{for } x<\varepsilon\\ u_0^+(x)+\varepsilon^2u_2^+(x)+\cdots+\varepsilon u_1^+(x)+\varepsilon^3u_3^+(x)+\cdots, & \text{for } x>\varepsilon\,.\end{cases} \tag{4.16}$$

Therefore, we see that the odd perturbation functions $u_{2K+1}(x)$ are antisymmetric about $x=0$, while the even perturbation functions $u_{2K}(x)$ are symmetric about the origin. Combining these symmetry conditions with (4.14) we see, for example, that

$$u_1^-(0)=-u_0^{-\prime}(0)\,, \tag{4.17a}$$

$$[u_1'(0)]=0\,, \tag{4.17b}$$

$$[u_0''(0)]=0\,. \tag{4.17c}$$

We observe that the compatability conditions (4.14) and the symmetry relations (4.17) place restrictions on the two-sided perturbation functions $u_i^\pm(x)$, which eliminate the extra freedom introduced into the representation (4.13).

The remaining conditions on the $u_i^\pm(x)$ come from the boundary-value problem (4.5) with $\partial u/\partial t=0$, namely,

$$\begin{aligned}0=u_\varepsilon''(x)-\omega^2u_\varepsilon(x)+\frac{f}{D}\\ +\frac{1}{D}\Bigg[\delta(x-\varepsilon)R(u_\varepsilon(x))\\ +\sum_{\substack{n=-N\\(n\neq0)}}^{N}\delta(x-x_n)R(u_\varepsilon(x))\Bigg]\,,\end{aligned} \tag{4.18}$$

here $\omega=(\Omega/D)^{1/2}$, together with boundary conditions (4.5b).

In order to determine the equations governing the perturbation functions u_K, we use the jump-condition form (2.3). We substitute (4.13) into the jump conditions obtained from (4.18), expand $u_K(\varepsilon)$ and $u_K'(\varepsilon)$ about $x=0$, expand R about $u_0(0)$ for the defect at $x=0$, expand R about $u_0(x_n)$ for the remaining defects in the lattice, and gather like powers of ε. In order to have a definite problem we choose $\varepsilon>0$ and pay due attention to the side of the representation (4.13) involved in the expansion process described above. The perturbation equations are

$$\varepsilon^0 > u_0''(x)+\omega^2 u_0(x)+\frac{f}{D}=0 ,$$

$$D[u_0'(x_n)]=-R(u_0(x_n)),\quad n=0,\pm1,\pm2,\ldots,\pm N ; \tag{4.19a}$$

$$\varepsilon^1 > u_1''(x)+\omega^2 u_1(x)=0 ,$$

$$D\{[u_0''(0)]+[u_1'(0)]\} = -R'(u_0(0))\{u_0^{-\prime}(0)+u_1^{-}(0)\} , \tag{4.19b}$$

$$D[u_1'(x_n)]=-R'(u_0(x_n))u_1(x_n),\ n=\pm1,\pm2,\ldots,\pm N;$$

$$\varepsilon^2 > u_2''(x)+\omega^2 u_2(x)=0 ,$$

$$D\{\tfrac{1}{2}[u_0''(0)]+[u_1''(0)]+[u_2'(0)]\} = -R'(u_0(0))\left[\frac{u_0''(0)}{2}+u_1'(0)+u_2(0)\right] + \frac{R''(0)}{2}[u_0^{-\prime}(0)+u_1^{-}(0)]^2 , \tag{4.19c}$$

$$D[u_2'(x_n)]=-R'(u_0(x_n))u_2(x_n) - \frac{R''(u_0(0))}{2}u_1^2(x_n),\ n=\pm1,\pm2,\ldots,\pm N.$$

a. Zeroth-order system. We observed that the zeroth-order system (4.19a) corresponds to the unperturbed periodic lattice. The solution to this system is given by (4.9a) in which we choose $\varepsilon=0$ and use periodic continuation to determine the solution throughout the domain $[-r,r]$. The stability of this solution is determined by the criterion given in (4.10a). In the case of the reactive-trapping model (4.8), $u_0(0)$ is given by (4.9b), and the stability criterion is given by (4.10b). The same physical interpretations of real and imaginary branches of (4.9b) hold.

b. First-order system. Combining the fact that $u_1(x)$ is antisymmetric about $x=0$ with the conditions (4.17), we see that the system (4.19b) on the interval $[0,r]$ can be rewritten as

$$u_1^{+\prime\prime}(x)+\omega^2 u_1^{+}(x)+\frac{R'(u_0(0))}{D}\sum_{n=1}^{N}\delta(x-x_n)u_1^{+}(x)=0 , \tag{4.20a}$$

together with the boundary conditions

$$u_1^{+}(0)=-u_0^{+\prime}(0) ,$$
$$u_1^{+\prime}(r)=0 . \tag{4.20b}$$

Notice that we have used the periodicity of $u_0(x)$ to write $R'(u_0(x_n))=R'(u_0(0))$. In the remainder of the analysis of the first-order system, we shall omit the superscript $+$ for u_1, i.e., $u_1^{+}\to u_1$.

As a matter of computational convenience, we assume that $N,r\to\infty$ so that we have an infinite lattice. If we make this assumption on the zeroth-order system, then our system would involve an infinite amount of material that is physically inadmissible. However, we expect the perturbation function u_1 to decay away from the perturbed point. In order that the perturbations should not involve an infinite amount of material, we assume that the perturbation function u_1 is absolutely integrable on $[0,\infty)$. This assumption has distinct computational advantages since (4.20) is reduced to solving a Dirichlet problem on the half-line.

In order to solve this problem we use the following Fourier sine transform pair:

$$\hat{u}_s(k)=\int_0^\infty \sin(kx)u(x)dx , \tag{4.21a}$$

$$u(x)=\frac{2}{\pi}\int_0^\infty \sin(kx)\hat{u}_s(k)dk . \tag{4.21b}$$

Applying the transform (4.21a) to (4.20) and inverting using (4.21b) we obtain

$$u_1(x)=-u_0^{+\prime}(0)e^{-\omega|x|} + \frac{R'(u_0(0))}{2\omega D} \times\sum_{n=1}^{\infty}(e^{-\omega|x-x_n|}-e^{-\omega|x+x_n|})u_1(x_n) . \tag{4.22}$$

Equation (4.22) expresses the solution $u_1(x)$ to (4.20) in terms of the values $u_1(x_n)$ at the defects. By choosing $x=x_m$, $m=0,\pm1,\ldots$ we obtain a summation equation (analogous to an integral equation) for the lattice point values $u_1(x_n)$. In fact, by letting $L\to0$ we could approximate (4.22) by an integral equation. However, we do not pursue the approximate solution in this limiting case, since it is possible to solve (4.22) using discrete Fourier transforms.

We define the discrete sine transform pair

$$f_S\{u_n\}=\bar{u}_s(\xi)=2L\sum_{n=1}^{\infty}u_n\sin(\xi x_n) ,$$
$$u_n=\frac{2}{\pi}\int_0^{\pi/2L}\bar{u}_s(\xi)\sin(\xi x_n)d\xi , \tag{4.23a}$$

and the discrete cosine transform pair

$$f_C\{u_n\}=\bar{u}_c(\xi)=Lu_0+2L\sum_{n=1}^{\infty}u_n\cos(\xi x_n) ,$$
$$u_n=\frac{2}{\pi}\int_0^{\pi/2L}\bar{u}_c(\xi)\cos(\xi x_n)d\xi . \tag{4.23b}$$

The discrete transforms (4.23) have the following combined convolution property:

$$\tilde{u}_s(\xi)\tilde{v}_c(\xi)=f_s\left[L\sum_{m=1}^{\infty}u_m(v_{n-m}-v_{n+m})\right] . \quad (4.24)$$

We now apply the finite sine transform (4.23a) to (4.22), use the convolution property (4.24), the definition of the cosine transform (4.23b), and the inversion formula given in (4.23a) to obtain the solution of (4.22):

$$u_1(x_n)=u_1(0)\theta^n , \quad (4.25)$$

where $\theta=\beta-(\beta^2-1)^{1/2}$ and

$$\beta=\cosh(\omega 2L)-\frac{R'(u_0(0))}{2\omega D}\sinh(2\omega L) .$$

It should be noted that the stability criterion (4.10a) guarantees that $\beta>1$, which ensures that $\theta<1$. It follows that $u_1(x_n)\to 0$ as $n\to\infty$, which is consistent with the boundary conditions (4.20b).

In what follows we will require an expression for $u_1'(0)$ in order to determine the perturbation to the desorption rate. By differentiating (4.22), letting $x\to 0^+$, and using the boundary condition (4.20b) we obtain

$$u_1'(0)=\omega u_0^{+\prime}(0)\left[1-\frac{R'(u_0(0))}{\omega D}\sum_{n=1}^{\infty}\theta^n e^{-\omega x_n}\right] . \quad (4.26)$$

c. Second-order system. The second-order system (4.19c) can be rewritten in the form

$$u_2''(x)+\omega^2 u_2(x)+\frac{R'(u_0(0))}{D}\sum_{n=-N}^{N}\delta(x-x_n)u_2(x)+\frac{1}{D}\sum_{n=-N}^{N}\delta(x-x_n)\alpha_n=0 , \quad (4.27)$$

where

$$\alpha_0=D\{[u_1''(0)]+\tfrac{1}{2}[u_0''(0)]\}+R'(u_0(0))\left[u_1'(0)+\frac{u_0''(0)}{2}\right] ,$$

$$\alpha_n=\frac{R''(u_0(0))}{2}u_1^2(x_n), \quad n=\pm 1,\pm 2,\ldots,\pm N .$$

Notice that we have used the periodicity of $u_0(x)$ to write $R'(u_0(x_n))=R'(u_0(0))$. We have also used (4.17a), which eliminates the R'' term from α_0, and (4.17b), which implies continuity of u_1' at $x=0$ and allows us to replace the negative branch $u_1^{-\prime}$ in (4.19c) by u_1'.

We again assume, as a matter of computational convenience, that we have an infinite lattice and that the perturbation function u_2 decays sufficiently rapidly away from the perturbation point to be absolutely integrable on $(-\infty,\infty)$. To solve (4.27) we use the following exponential Fourier transform pair:

$$\hat{u}(k)=\int_{-\infty}^{\infty}e^{-ikx}u(x)dx , \quad (4.28a)$$

$$u(x)=\frac{1}{2\pi}\int_{-\infty}^{\infty}e^{ikx}\hat{u}(k)dk . \quad (4.28b)$$

Taking the Fourier transform of (4.27) and inverting using (4.28b), we obtain

$$u_2(x)=\frac{R'(u_0(0))}{2\omega D}\sum_{n=-\infty}^{\infty}u_2(x_n)e^{-\omega|x-x_n|}+\frac{1}{2\omega D}\sum_{n=-\infty}^{\infty}\alpha_n e^{-\omega|x-x_n|} . \quad (4.29)$$

Equation (4.29) expresses the solution $u_2(x)$ to (4.27) in terms of the values $u_2(x_n)$ at the defects. The values $u_2(x_n)$ at the defects can be determined by letting $x=x_m$ in (4.29) and by solving the resulting summation equation. This summation equation reduces to an integral equation in the limit $L\to 0$.

In order to solve the summation equation (4.29), we introduce the following exponential transform pair:

$$f_e\{u_n\}(\xi)=\tilde{u}_e(\xi)=2L\sum_{n=-\infty}^{\infty}e^{-i\xi x_n}u_n , \quad (4.30a)$$

$$u_n=\frac{1}{2\pi}\int_{-\pi/2L}^{\pi/2L}e^{i\xi x_n}\tilde{u}_e(\xi)d\xi . \quad (4.30b)$$

The discrete exponential transform (4.30) has the following convolution property:

$$\tilde{u}_e(\xi)\tilde{v}_e(\xi)=f_e\left[2L\sum_{m=-\infty}^{\infty}u_m v_{n-m}\right](\xi) . \quad (4.31)$$

Taking the discrete exponential transform of (4.29) and exploiting the convolution property (4.31) we obtain

$$f_e\{u_2(x_n)\}(\xi)=\frac{\sinh(2\omega L)f_e\{\alpha_n\}(\xi)}{2\omega D[\beta-\cos(2\xi L)]} , \quad (4.32)$$

where β is defined in (4.25).

To obtain the solution $u_2(x_n)$ to (4.29) we can apply the inversion formula (4.30b). However, for our purposes in what follows, it suffices to determine $\sum_{n=-\infty}^{\infty}u_2(x_n)$. Since $u_2(x_n)$ is absolutely summable, we observe from (4.30) that the above summation can be evaluated directly by considering $f_e\{u_2(x_n)\}(0)/2L$, which can be determined by letting $\xi=0$ in (4.32). Following this procedure we obtain

$$\sum_{n=-\infty}^{\infty}u_2(x_n)=\frac{\sum_{n=-\infty}^{\infty}\alpha_n}{2\omega D\tanh(\omega L)-R'(u_0(0))} . \quad (4.33)$$

3. *The perturbation to the desorption rate*

The ultimate objective of this analysis is to determine the influence of perturbing the defect at $x=0$ on the desorption rate $\mathcal{D}$. We use the expression (4.7) to determine the perturbed desorption rate $\mathcal{D}(\varepsilon)$:

$$\mathcal{D}(\varepsilon)=\mathcal{D}_0+\varepsilon\mathcal{D}_1+\varepsilon^2\mathcal{D}_2+\cdots \quad (4.34a)$$

$$=f+\frac{1}{2r}\left[R(u_\varepsilon(\varepsilon))+\sum_{\substack{n=-N\\(n\neq 0)}}^{N}R(u_\varepsilon(x_n))\right] . \quad (4.34b)$$

Following the same procedure used in (4.18) to expand $R(u_\varepsilon(x))$ about the points $x=0,\pm 2L,\ldots,$ we obtain

the following expressions for $\mathcal{D}_k$:

$$\mathcal{D}_0=f+\frac{1}{2r}\sum_{n=-N}^{N}R(u_0(x_n))\,,$$

$$\mathcal{D}_1=\frac{R'(u_0(0))}{2r}\left[u_0^{-\prime}(0)+u_1^{-}(0)+\sum_{\substack{n=-N\\(n\neq 0)}}^{N}u_1(x_n)\right],$$

$$\mathcal{D}_2=\frac{R'(u_0(0))}{2r}\left[\frac{u_0^{-\prime\prime}(0)}{2}+u_1^{-\prime}(0)+\sum_{n=-N}^{N}u_2(x_n)\right]+\frac{R''(u_0(0))}{4r}\left[\{u_0^{-\prime}(0)+u_1^{-}(0)\}^2+\sum_{\substack{n=-N\\(n\neq 0)}}^{N}u_1^2(x_n)\right], \tag{4.35}$$

$\cdots$.

We observe that $\mathcal{D}_0$ is the unperturbed desorption rate. Using the condition (4.17a) and the antisymmetry of $u_1(x)$ we see that $\mathcal{D}_1=0$. This demonstrates that the perturbation to the desorption rate does not depend on the side to which the defect is perturbed, which is consistent with physical intuition.

In order to use (4.26) and (4.33), which were derived assuming an infinite periodic lattice of defects, we assume that $r,N\gg 1$. In this case the error committed by using these infinite surface formulas is negligibly small.

Using the condition (4.17a), the antisymmetry of $u_1(x)$ about $x=0$, and substituting (4.26) and (4.33) into (4.35) we obtain

$$2r\mathcal{D}_2\simeq\frac{R'}{T-R'}\left[D\{[u_1''(0)]+\tfrac{1}{2}[u_0'''(0)]\}+\tfrac{1}{2}Tu_0''(0)+T\omega u_0^{+\prime}(0)\left[1-\frac{R'}{\omega D}\sum_{n=1}^{\infty}\theta^n e^{-\omega x_n}\right]\right]+\frac{\{u_0^{+\prime}(0)\}^2TR''}{T-R'}\sum_{n=1}^{\infty}\theta^{2n}\,, \tag{4.36}$$

where $T=2\omega D\tanh(\omega L)$, $R'=R'(u_0(0))$, and $R''=R''(u_0(0))$. The approximate equality $\simeq$ results from the infinite lattice approximation.

We now use the fact that the perturbation functions $u_0(x),\ldots$ satisfy the differential equations in (4.19a),... respectively, the jump-condition form (2.3), the nonlinear equation (3.3b) which is satisfied by $u_0(0)$, and then sum the series in (4.36) to obtain

$$2r\mathcal{D}_2\simeq\frac{R'R\omega^2}{T-R'}\times\left\{1-\tanh(\omega L)\left[1-\frac{R'}{\omega D}\left[\frac{e^{-2\omega L}\theta}{1-e^{-2\omega L}\theta}\right]\right]\right\}+\frac{TR''R^2}{4D^2(T-R')}\frac{\theta^2}{1-\theta^2}\,. \tag{4.37}$$

In Sec. IV B 1 we consider a single defect to be embedded into a periodic lattice of defects in which symmetry-breaking perturbations to the defect were assumed not to affect the solution in the lattice. Equation (4.37) is an expression for the perturbation to the desorption that includes the effects of the entire lattice of defects. Comparing (4.11b) with (4.37) we see that when the effects of the lattice of defects are included, a $\tanh(\omega L)$ is replaced by the term in square brackets in (4.37) and an additional term appears that depends on the curvature R'' of R at the unperturbed defect concentration $u_0(0)$.

We now consider the effect on the desorption rate of perturbing a single defect in a periodic lattice. If $\mathcal{D}_2$ is positive (negative) then the desorption rate is increased (decreased) by perturbing the defect.

In the analysis that follows, we assume that we are considering perturbations to the stable steady states associated with reactive trapping by defects. Therefore, applying the stability criterion (4.10) we observe that in (4.37),

$$T-R'>0\,. \tag{4.38}$$

Applying the property (R5), the fact that $\theta<1$ for a stable system, and (4.38) we observe that the second term in (4.37) is always positive. We observe the following properties of the expression for $\mathcal{D}_2$ given in (4.37).

(I) For values of $u_0(0)\in(0,u_C)$, $\mathcal{D}_2>0$. To demonstrate this result we consider the sign of the first term in (4.37) when $u_0(0)\in(0,u_C)$. According to (R4), $R'<0$ for this range of values of $u_0(0)$. Now define $\mathcal{E}$ to be the expression in curly brackets in (4.37), namely,

$$\mathcal{E}(\omega L,\alpha)=1-\tanh(\omega L)\left[1+\frac{2\alpha e^{-2\omega L\theta}}{1-e^{-2\omega L\theta}}\right], \tag{4.39}$$

where $\alpha=|R'|/2\omega D$ and we have used the fact that $R'<0$. We now look for the roots of $\mathcal{E}$, which can be shown to be given by the solution of

$$\alpha[(1+\alpha)e^{4\omega L}-2\alpha e^{2\omega L}-(1-\alpha)]=0\,. \tag{4.40}$$

We observe that $\mathcal{E}$ is zero when

$$\alpha=0\,, \tag{4.41a}$$

$$e^{2\omega L}=1\,, \tag{4.41b}$$

$$e^{2\omega L}=1-\frac{2}{1+\alpha}\,. \tag{4.41c}$$

From (4.41a) we see that $\mathcal{E}$ has a root when $R'=0$, which does not occur in the interval $(0,u_C)$. From (4.41b) we see that $\mathcal{E}$ has a root when $\omega L=0$. This root corresponds to an infinite number of defects in which case $u_0(0)=0\notin(0,u_C)$. Since $\infty>\alpha>0$ we see that (4.41c) has no solution for positive (i.e., physically admissible) values of ωL. Therefore, we conclude that $\mathcal{E}$ has no roots for $u_0(0)\in(0,u_C)$. We also note that the root (4.41b) is associated with the end point $u=0$ of the interval, while the root (4.41a) is associated with the end point u_C. Since the interval $(0,u_C)$ is open these points are not included.

Since $\mathcal{E}$ has no roots in $(0,u_C)$ we need only determine the sign of $\mathcal{E}$ at one point in the interval $(0,u_C)$. We achieve this by considering the limiting case $0<-R'/2\omega D=\alpha\ll 1$, for which

$$\mathcal{E} \sim 2e^{-2\omega L}\left[\frac{1+\alpha(1+\alpha^2)e^{-2\omega L}-(1-\alpha)^2 e^{-4\omega L}}{1+e^{-2\omega L}-(1-\alpha)e^{-4\omega L}-(1-\alpha)e^{-6\omega L}}\right]. \tag{4.42}$$

This expression is positive, provided that $0<\omega L<\infty$. We conclude, therefore, that $u\in(0,u_C)$ implies that $\mathcal{E}>0$. Since both R and R' are negative on $(0,u_C)$ we conclude that $\mathcal{D}_2>0$ on $(0,u_C)$.

(II) For values of $u_0(0)\in(u_C,u_S)$, $\mathcal{D}_2$ may be positive or negative. However, for values of $u_0(0)$ remote from the critical point u_C, $\mathcal{D}_2<0$. From (4.37) it can be seen that when $R'>0$ the term in the curly brackets is always positive. Therefore, the first term in (4.37) is then always negative. The sign of $\mathcal{D}_2$ now depends upon the relative magnitudes of the first and second terms in (4.37). In order to demonstrate a regime of desorption in which $\mathcal{D}_2<0$ assume the following: we have a relatively large value of adsorption f that admits a steady-state defect concentration $u_0(0)\in(u_C,u_S)$ for large values of ωL, which is not close to u_C, i.e., $R'(u_0(0))\gg e^{-2\omega L}$. For $\omega L\gg 1$, we have

$$2r\mathcal{D}_2 \sim \frac{R'R\omega^2}{T-R'}\left[2e^{-2\omega L}+\frac{R'e^{-4\omega L}}{1-R'}+\cdots\right] + \frac{TR''R^2}{4D^2(T-R')}\left[\frac{e^{-4\omega L}}{1-R'}+\cdots\right]. \tag{4.43}$$

We observe that provided the curvature $R''(u_0(0))$ is bounded, the first term will dominate when $\omega L\gg 1$. Since $R'>0$ and $R<0$ we conclude that $\mathcal{D}_2<0$.

In Fig. 4 we illustrate the various regimes of desorption for a periodic lattice of defects using the simple reactive-trapping model (4.8). $2r\mathcal{D}_2$ as given by (4.37) is plotted as a function of L assuming that the other parameter values are fixed at the values $D=1.0$, $f=1.4$, $\Omega=2.0$, and $\gamma=1.0$. By allowing L to increase we are effectively increasing the steady-state defect concentration $u_0(0)$. This allows both intervals (I) $u_0(0)\in(0,u_C=\frac{1}{2})$ and (II) $u_0(0)\in(u_C,u_S=1)$ to be accessed and the behavior of $\mathcal{D}_2$ to be observed. In order to see the relationship between $\mathcal{D}_2$ and R', R' is also plotted in Fig. 4 in the vicinity of the value of $L=0.3356$ at which R' changes sign.

In Fig. 4 the perturbation $\mathcal{D}_2$ to the desorption is clearly positive in the region (I) $0<L<0.3356$ within which the gradient R' is negative. Within the region (II) $0.3356<L<2.0$, $\mathcal{D}_2$ is initially positive and small [consistent with the first term of (4.37) vanishing at $u_0(0)=u_C$] after which $\mathcal{D}_2$ becomes negative and exhibits the asymptotic behavior predicted by (4.43) as L increases.

It is interesting to note that $\mathcal{D}_2$ reaches a maximum value at about $L=0.1$. Physically this implies that in the range $0<L<0.1$, there is such a high density of defects that the perturbation of just one defect starts to lose its dominant effect as L is decreased.

4. Comments

We have considered a class of continuum models representing reactive trapping by defects. We investigated the influence of defect locations on the balance between desorption associated with defects (which we referred to as reactive trapping) and bulk desorption (which we referred to as desorption). In order to analyze the effect of defect locations, we considered symmetry-breaking perturbations to a single defect in a periodic lattice and measured the effect on the desorption rate.

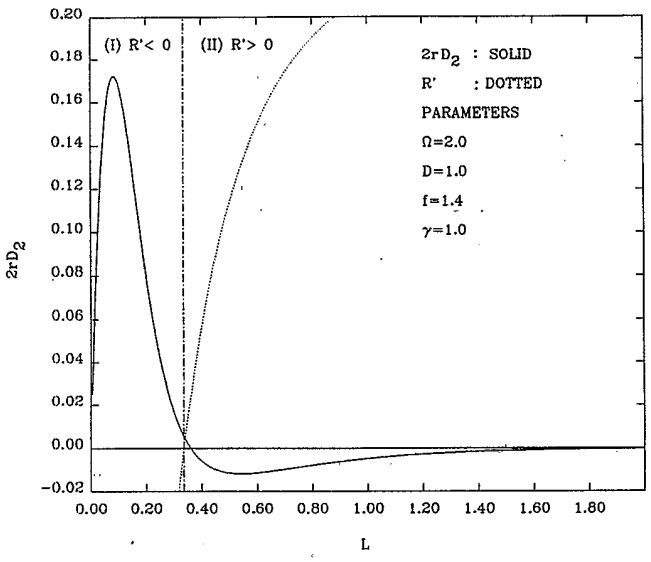

FIG. 4. The function $2r\mathcal{D}_2$ represents the perturbation to the desorption when the effects of all the defects in the periodic lattice are included. We notice that in region (I) $R'<0$ and $\mathcal{D}_2>0$. In region (II) $\mathcal{D}_2$ is initially small and positive in the vicinity of the critical point at which $R'=0$. Away from this point $\mathcal{D}_2$ is clearly negative with an asymptotic behavior given by (4.43).

For the class of reactive-trapping models (R1)–(R5) it is possible to identify two regimes of desorption. In the region in which $R'(u)<0$, competitive behavior between the two defects that are moved closer together by the perturbation reduces the trapping efficiency of the lattice of defects as a whole, and the bulk desorption rate increases. In the region in which $R'(u)>0$ the desorption rate may be either increased or decreased by perturbing a defect. However, for nominal values of u which are remote from the critical point u_C: $R'(u_C)=0$, the bulk desorption rate can be shown to decrease as a result of perturbing a defect. In this regime, the defects that are moved closer together by the perturbation exhibit cooperative behavior. Each reduces the access limitation or saturation level of the other, which enhances the trapping efficiency of the lattice of defects as a whole.

These interesting phenomena may at first sight seem intuitively obvious. However, the following argument might be made for either enhanced or reduced competitiveness to occur: The defect that is moved by the perturbation is moved closer to one of its neighbors and farther from the other. This defect will experience enhanced competition with its nearer neighbor and reduced competition with the farther neighbor. It is in this situation of competing effects that a detailed quantitative account

of all the opposing physical processes is necessary in order to decide which dominates. Therefore, without an analysis such as that presented in this section, it would be extremely difficult to determine which of the intuitively predictable processes dominate in this nonlinear environment.

If small *random* perturbations of the order of ε were made to the locations of *all* the defects, then the equations governing the perturbation functions $u_1(x)$ and $u_2(x)$ would be of the same form as (4.19b) and (4.19c), respectively. Since these equations are linear, the solutions $u_1(x)$ and $u_2(x)$ can be expressed as a superposition of solutions in which each defect is perturbed one at a time. The perturbations to the desorption rate could then be expressed in terms of the single-defect perturbation functions. The importance of this superposition property is that we can expect similar competitive and cooperative behavior when all the defects undergo small perturbations.

If we consider the steady bulk desorption rate to be a function of the locations of the defects, then in the regime $R'(u)<0$ the uniform spacing of defects is a local minimum of this desorption rate function. The fact that we have only identified a local minimum is due to the assumption of small perturbations. We shall investigate the issue of finite perturbations and global minima numerically in the next section.

Since only the requirement (R1) [that $R(u)$ be analytic] is formally fundamental to the analysis, the analysis procedure outlined could be applied to investigate the effect of defect locations in other physical situations. The properties (R2)–(R5) used to build the features of reactive trapping by defects into the model are by no means exhaustive. Other features that could be included are, for example, multiple cycles of enhanced trapping and access limitation provided that the fundamental requirement (R1) is retained. However, the model already treated encompasses all the anticipated basic physics. The same techniques could be applied to the case of more complex chemistry with several species.

V. THE DESORPTION RATE FOR A RANDOM DISTRIBUTION OF DEFECTS–FINITE PERTURBATIONS

In Sec. IV we identified a regime of desorption from a surface with a periodic array of defects in which a small perturbation to one of the defects caused an increase in the rate of bulk desorption from the surface. Therefore, by regarding the bulk desorption rate as a function of the defect locations, we see that the uniform spacing of a given number of defects is a local minimum of the function. It is natural for realistic practical situations to consider the effect of finite perturbations and the issue of a global minimum of the desorption function for a given number of defects.

The problem of finite perturbations requires numerical calculations. The implementation and convergence of the boundary-element (BE) technique for solving linear diffusion problems with localized nonlinear reactions has been discussed by the current authors.[13,14] We use the BE technique to determine the steady desorption rate when the defects are randomly distributed throughout the surface. For the purposes of this study we use the simple reactive-trapping model (4.8).

A. Finite perturbations in the competitive regime

We consider an array of ten defects that fall in the competitive regime when they are distributed uniformly throughout the interval [0,2]. In this case the interdefect spacing is $2L=0.2$, while the other parameters defined in Sec. IV are $\Omega=2.0$, $D=1.0$, $f=2.0$, and $\gamma=1.0$. This parameter set for the uniformly distributed array of defects is precisely that used in Sec. IV B 1 to demonstrate competitive behavior between neighboring defects. The unperturbed solution and the solution assuming a small perturbation in the single-defect case is shown in Fig. 3(a). In terms of the critical adsorption level f_c, this parameter set corresponds to the competitive regime denoted in Fig. 3(c) by a square symbol. The unperturbed desorption rate for this parameter set is $\mathcal{D}(0)=0.8027$.

We now introduce finite random perturbations to the defect locations and determine the corresponding bulk desorption rate $\mathcal{D}$ using the BE technique. In Fig. 5 the steady-state concentration profile across the interval [0,2.0] is plotted in the case of evenly spaced defects and a particular random selection of defects. The locations of the randomly spaced defects are indicated in Fig. 5 by solid circles. The desorption rate in the case of the finite

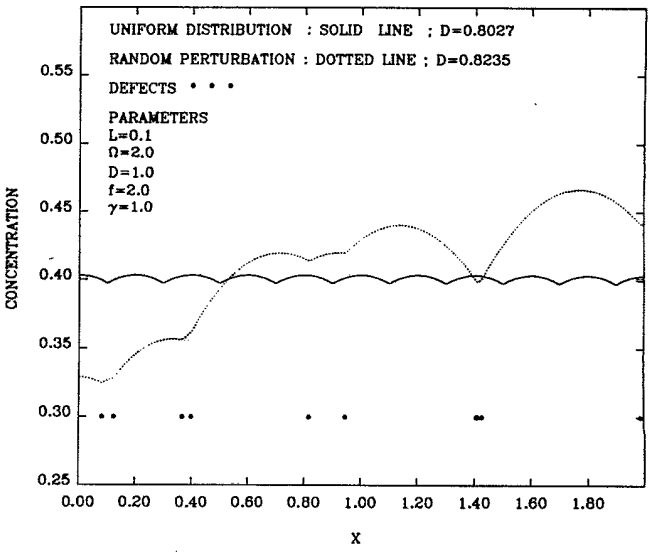

FIG. 5. The steady-state concentration profile for a uniformly spaced set of ten defects is plotted with a solid line. These defects are assumed to undergo finite random perturbations and the steady-state concentration profile is plotted with a dotted line. The location of the random defects are denoted by the solid circles. The small perturbation theory predicts that the uniform defects are in the *competitive* regime. Thus the desorption rate is expected to increase. The desorption rate *increased* from $\mathcal{D}=0.8027$ for the uniform distribution to $\mathcal{D}=0.8235$ for the randomly perturbed defects. Thus the competitive behavior persists even when there are finite perturbations.

random perturbations increased to the value of 0.8235. Thus even finite perturbations to defects in the competitive regime cause the bulk desorption rate to increase.

In order to establish whether this is an isolated incident the perturbation procedure was repeated 800 times with a different random defect distribution in each case. The average bulk desorption rate for all these random defect distributions was 0.8457. In Fig. 6(a) the frequency distribution of the desorption rates of all the defect distributions is plotted. For reference the uniform desorption level $\mathcal{D}(0)$ is denoted by the triangular symbol. From the enlargement plotted in Fig. 6(b) it can be seen clearly that there was no incidence of a defect distribution below $\mathcal{D}(0)$.

Although this random sampling method does not provide a proof that the periodic spacing is a global minimum, it does provide statistical evidence for this claim.

B. Finite perturbations in the cooperative regime

We consider an array of five defects that fall in the cooperative regime when they are evenly distributed throughout the interval [0,2.0]. In this case the interdefect spacing is $2L=0.4$, while the other parameters defined in Sec. IV are $\Omega=2.0$, $D=1.0$, $f=2.0$, and $\gamma=1.0$. The parameter set for this uniformly spaced array of defects is that used in Sec. IV B 1 to demonstrate cooperative defect behavior. The unperturbed solution and the solution assuming a small perturbation in the single defect case are shown in Fig. 3(b). In terms of the critical adsorption level f_c, this parameter set corresponds to the cooperative regime denoted in Fig. 3(c) by a solid circle. The unperturbed desorption rate for this parameter set is $\mathcal{D}(0)=1.5701$.

As was done in the previous case we introduce finite random perturbations to the defect locations and determine the corresponding steady solution and desorption rate using the BE technique. In Fig. 7 the steady-state concentration profile across the interval [0,2.0] is plotted in the case of uniformly spaced defects and in the case of a particular random selection of defects. The locations of the defects are indicated in Fig. 7 by solid circles. The desorption rate in this case of finite random perturbations is decreased to the value $\mathcal{D}=1.4614$. This is consistent with the fact that defects that are moved closer together act cooperatively to reduce the local saturation level so the bulk desorption rate decreases. This result demonstrates that the defects still operate in the cooperative regime even when the defects undergo finite perturbations.

In order to establish whether this is an isolated incident, the perturbation procedure was repeated 400 times with different random defect spacing in each case. The average bulk desorption rate for all these random defect distributions was 1.4572. In Fig. 8 the frequency distribution of the desorption rates of all the random defect distributions is plotted. For reference the uniform desorption level $\mathcal{D}(0)=1.5701$ is denoted by the triangular symbol. It can be seen that there was no incidence of a defect distribution above $\mathcal{D}(0)$. This indicates that the cooperative behavior that was established theoretically in the small perturbation case persists even when the defects are subjected to finite random perturbations.

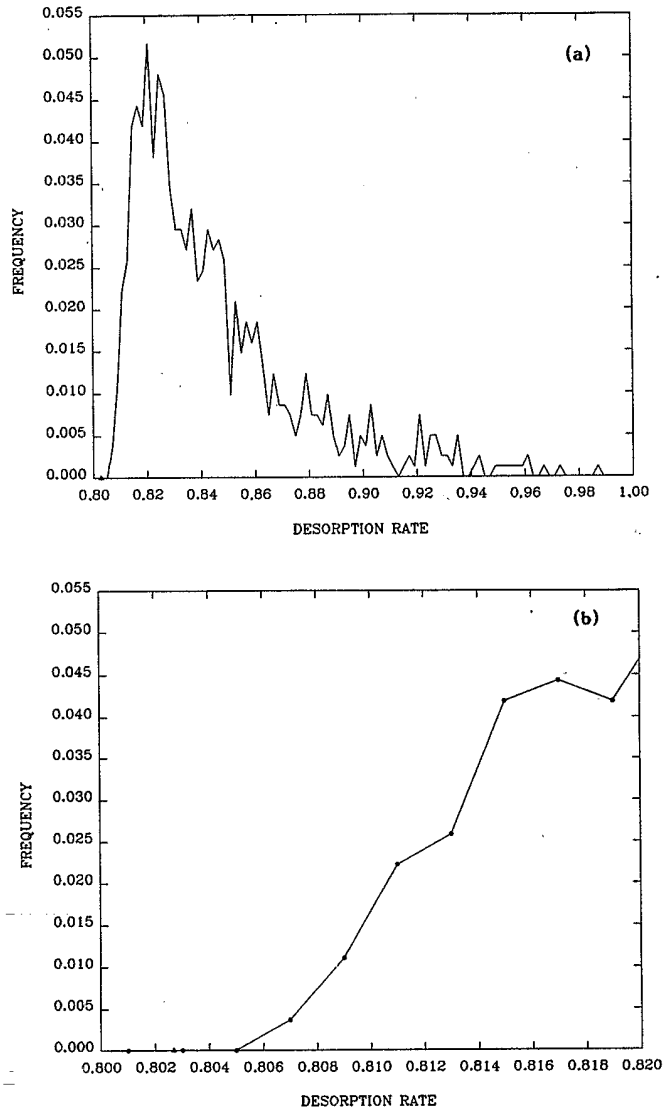

FIG. 6. (a) The frequency distribution of the desorption rate $\mathcal{D}$ is plotted for 800 different perturbation cases. We use the same parameter set as that in Fig. 5 so that the ten uniformly spaced defects are in the competitive mode. The desorption rate $\mathcal{D}(0)=0.8027$ for the uniform distribution of defects is indicated by a triangular symbol. Clearly there was no incidence of a perturbed defect set that had an associated desorption rate that was lower than $\mathcal{D}(0)$. This provides statistical evidence for the claim that the desorption rate is a global minimum when the defects are evenly spaced. (b) The frequency plot in (a) is enlarged in the vicinity of the desorption rate $\mathcal{D}(0)$ of the evenly spaced defects. The triangular symbol indicates the level of $\mathcal{D}(0)$ of the uniformly spaced defects. The circular symbols indicate the frequency at the midpoints of the sampled intervals.

VI. COMMENTS AND CONCLUSION

We have considered the linear diffusion equation with localized nonlinear reactions. This class of equation has

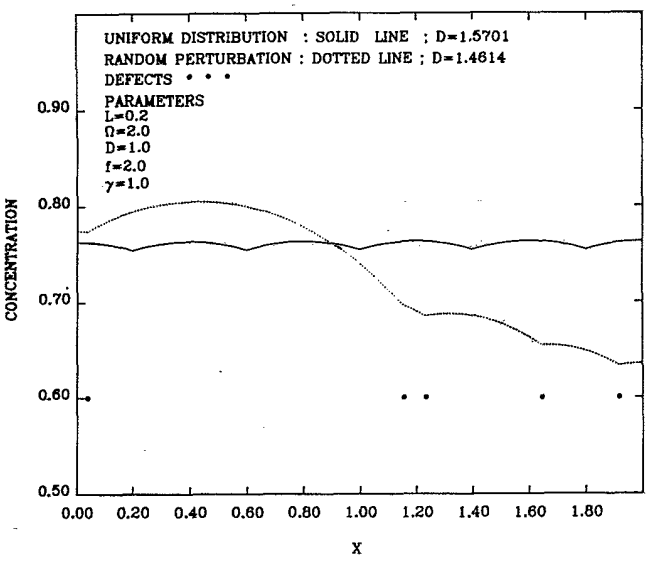

FIG. 7. The steady-state concentration profile for a uniformly spaced set of five defects is plotted with a solid line. These defects are assumed to undergo finite random perturbations and the steady-state concentration profile is plotted with a dotted line. The locations of the random defects are denoted by solid circles. The small perturbation theory predicts that the uniformly spaced defects are in the *cooperative* regime so we expect the desorption rate to decrease. The desorption rate *decreased* from $\mathcal{D}(0)=1.5701$ for the uniform distribution to $\mathcal{D}=1.4614$ for the randomly perturbed defects. Thus the cooperative behavior persists even when there are finite perturbations.

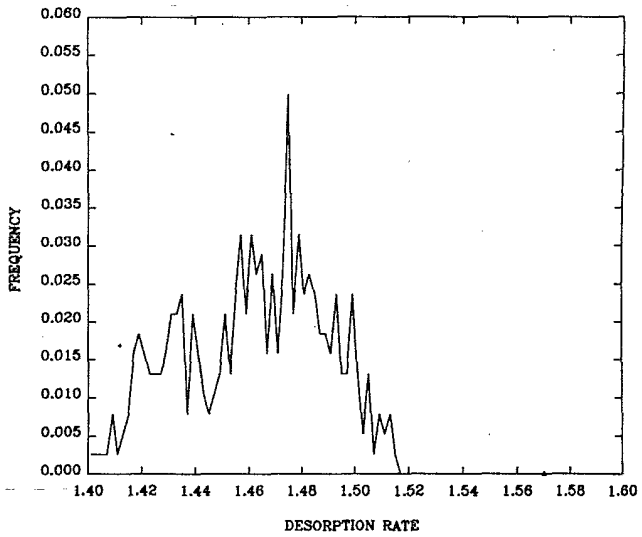

FIG. 8. The frequency distribution of the desorption rate $\mathcal{D}$ is plotted for 400 different perturbation cases. We use the same parameter set as that in Fig. 7 so that the five uniformly distributed defects are in the cooperative mode. The desorption rate $\mathcal{D}(0)=1.5701$ for the uniform spacing of defects is indicated by a triangular symbol. There is no incidence of a perturbed defect set for which the desorption rate was larger than $\mathcal{D}(0)$. This provides statistical evidence that the cooperative phenomenon established by the small perturbation theory persists when finite random perturbations are applied.

been considered by a number of authors in the context of membrane bound enzymes,[9–11] cooperative instability phenomena in arrays of catalytic sites,[8] and enzyme particles in stirred reacting fluids.[12] We have considered the diffusion-localized-reaction equation in the context of a continuum approximation to study the effect of defect sites on a catalytic surface.

We have outlined a novel procedure that uses conformal mapping to determine sufficient conditions for linear stability of steady states. This technique enables one to reduce the complex problem of determining conditions under which roots of a transcendental equation lie in the region $\mathrm{Re}(s)<0$ to that of determining conditions under which a polynomial equation has roots in a transformed stability region. In addition to being able to derive stability criteria for given situations, the technique provides useful insight into the way in which the various physical processes influence stability by altering the slope and extent of the stability region. The procedure was introduced by means of some simple examples, and we discussed the manifestation of the various physical processes by the way they deform the various stability regions. Using this technique it was possible to derive stability criteria that were used later in the paper.

We considered a class of models in which a process of reactive trapping with eventual saturation is assumed to take place at defects. In the context of such models, we assessed the continuum assumption by comparing the continuum approximation to the steady states of a discrete defect model. The continuum approximation is already seen to be remarkably good even when the number of sites between defects is as low as 20.

Having validated the continuum model, we used it to analyze the effect of the distribution of defects on a surface upon the desorption processes on the surface. In particular, we considered the effect of small symmetry-breaking perturbations to the defects in a periodic array on the balance between the desorption processes taking place on the surface.

A number of interesting phenomena were observed.

(i) Competitive behavior. There is a regime in which competitive behavior occurs between defects that are moved closer by perturbation. This reduces the trapping efficiency of the lattice of defects as a whole and the bulk desorption rate increases as a result. If the desorption rate is regarded as a function of the defect locations, then the uniform distribution of defects forms a local minimum of this desorption function.

(ii) Cooperative behavior. A regime of cooperative behavior can be identified in which defects that are moved closer by the perturbation mutually reduce the saturation effect locally. This increases the trapping efficiency of the lattice of defects as a whole, and the bulk desorption decreases as a result. Near critical points of the reactive-trapping model, we demonstrated that cooperative behavior does not necessarily dominate the perturbations to the desorption process.

If physical intuition is used to attempt to predict the

effect of such perturbations, then it is likely that ambiguous conclusions will arise. This stems from the fact that there are a number of competing physical effects that could make the desorption rate increase or decrease. Thus an analysis is required which provides a detailed quantitative account of all the competing physical processes in this nonlinear environment in order to determine which process dominates. We outlined a procedure which enables one to identify the dominant physical processes, and to identify features of the reactive-trapping model that determine the regime of desorption in a given situation. This procedure makes use of a two-sided perturbation representation, which introduces more freedom into the representation than can be determined by the governing differential equation and boundary conditions alone. This additional freedom is removed by requiring that the solution be continuous and that the representation satisfy appropriate symmetry conditions. This device allows us to obtain the correct expansions in the vicinity of the singular points at which the derivative of the solution is discontinuous. It also enables us to take advantage of the symmetry of the periodic lattice in order to solve the perturbation equations order by order.

This procedure is quite general in that it applies for a large class of reactive-trapping models and can also be used to analyze situations in which different physical processes take place at the defects. The perturbation procedure can also be extended to analyze the effect of symmetry-breaking deformations to defect manifolds in dimensions greater than one.

We investigated numerically the effect of finite random perturbations to defect locations on the bulk desorption rate using the boundary-element technique. An illustration was provided in which the effect of finite random perturbations to a uniform lattice in the competitive regime still increased the bulk desorption rate. By performing a large number of such finite random perturbations, statistical evidence was provided for the claim that the desorption rate considered as a function of the defect locations has a global minimum when the defects are evenly spread. A similar experiment was performed for the cooperative regime in which the findings of the small perturbation analysis were also corroborated.

These analytical and numerical investigations of the properties of the continuum model of defects on surfaces have led to the identification of interesting competitive and cooperative phenomena. The current study also demonstrates the usefulness of such continuum models in that they provide access to powerful analytic tools that can be applied to the problem. Similar nonlinear competing effects were found to operate in cases of active site poisoning of catalytic surfaces.[5]

The same class of reactive-trapping defect reactions have been investigated numerically for defect structures on two-dimensional surfaces.[13] The effect of changes in defect geometry on the balance between the desorptive processes were explored in that study. A richer class of competitive and cooperative phenomena occurred in the case of the two-dimensional defect structures than occurred in the case of the one-dimensional defect arrays considered in this paper. First, strong intrinsic competition occurred for circular defect structures that formed islands of nearly constant concentration. Second, material along V-shaped defect structures was found to be distributed in a way that reflects the relative competitiveness of defects on opposite sides of the defect structure. The phenomenon of maximum competitiveness demonstrated in Fig. 4 also occurred in the case of V-shaped defect structures. The V-shaped defect structures exhibited a region of maximal competitiveness away from the vertex along the axis of symmetry. Third, in two dimensions, defect distributions that are less regular in shape were found to be less competitive than defect structures which had the same defect length but which had greater symmetry.

ACKNOWLEDGMENTS

The authors acknowledge support for this research from the U.S. Office of Naval Research and the U.S. Air Force Office of Scientific Research. The first author also gratefully acknowledges the support of the Council of Scientific and Industrial Research (CSIR) of South Africa and the Fulbright Foundation.

[1]J. A. Serri, J. C. Tully, and M. J. Cardillo, J. Chem. Phys. **79**, 1530 (1985).
[2]D. L. Freeman and J. C. Doll, J. Chem. Phys. **78**, 6002 (1983); **79**, 2343 (1983).
[3]R. I. Cukier, J. Chem. Phys. **79**, 2430 (1983).
[4]F. F. Grinstein, H. Rabitz, and A. Askar, J. Chem. Phys. **82**, 3430 (1985).
[5]D. Lee, A. Askar, and H. Rabitz (unpublished).
[6]E. K. Bimpong-Bota, P. Ortoleva, and J. Ross, J. Chem. Phys. **60**, 3124 (1974).
[7]R. M. Shymko and L. Glass, J. Chem. Phys. **60**, 835 (1974).
[8]E. K. Bimpong-Bota, A. Nitzan, P. Ortoleva, and J. Ross, J. Chem. Phys. **66**, 3650 (1977).
[9]L. Glass and S. A. Kauffman, J. Theor. Biol. **34**, 219 (1972).
[10]H. D. Thames, J. Theor. Biol. **41**, 331 (1973).
[11]H. D. Thames and A. D. Elster, J. Theor. Biol. **59**, 415 (1976).
[12]J. C. M. Lee and D. Luss, Am. Inst. Chem. Eng. J. **10**, (1970).
[13]A. Peirce and H. Rabitz, Surf. Sci. (to be published).
[14]A. Peirce, A. Askar, and H. Rabitz (unpublished).
[15]J. J. Tyson and J. C. Light, J. Chem. Phys. **59**, 4164 (1973).
[16]E. J. Watson, *Laplace Transforms and Applications* (Van Nostrand Reinhold, New York, 1981).